INFORMATION TO USERS

This manuscript has been reproduced from the microfilm master. UMI films the text directly from the original or copy submitted. Thus, some thesis and dissertation copies are in typewriter face, while others may be from any type of computer printer.

The quality of this reproduction is dependent upon the quality of the copy submitted. Broken or indistinct print, colored or poor quality illustrations and photographs, print bleedthrough, substandard margins, and improper alignment can adversely affect reproduction.

In the unlikely event that the author did not send UMI a complete manuscript and there are missing pages, these will be noted. Also, if unauthorized copyright material had to be removed, a note will indicate the deletion.

Oversize materials (e.g., maps, drawings, charts) are reproduced by sectioning the original, beginning at the upper left-hand corner and continuing from left to right in equal sections with small overlaps.

Photographs included in the original manuscript have been reproduced xerographically in this copy. Higher quality 6" x 9" black and white photographic prints are available for any photographs or illustrations appearing in this copy for an additional charge. Contact UMI directly to order.

ProQuest Information and Learning
300 North Zeeb Road, Ann Arbor, MI 48106-1346 USA
800-521-0600

Université d'Ottawa · University of Ottawa

Kinetic Study of the Stabilization and Reduction of the Aqueous Mercuric Ion by Sulfite: Implications for Atmospheric Deposition

Lisa L. Van Loon

Thesis submitted to the School of Graduate Studies and Research
University of Ottawa
in partial fulfillment of the requirements for the degree of

Master of Science
in
Chemistry
Chemical and Environmental Toxicology

in the Ottawa-Carleton Chemistry Institute,
Department of Chemistry
University of Ottawa
Ottawa, Ontario
Canada

Lisa L. Van Loon	Dr. Susannah L. Scott
M. Sc. Candidate	Research Supervisor

Abstract

In aqueous solution, Hg^{2+} forms both 1:1 and 1:2 complexes with the sulfite anion. $Hg(SO_3)_2^{2-}$ is redox-stable, but when one SO_3^{2-} ligand dissociates, the redox-unstable $HgSO_3$ is generated. With $Hg^{2+}_{(aq)}$ in excess, $HgSO_3$ was observed for the first time. This complex undergoes a highly temperature sensitive intramolecular redox reaction which is kinetically first-order. The activation parameters are consistent with a unimolecular bond cleavage.

In the presence of excess sulfite, $Hg(SO_3)_2^{2-}$ is formed. Under these conditions, the rate of reduction of $Hg^{2+}_{(aq)}$ to Hg^0 depends inversely on the concentration of uncoordinated sulfite, yet remains unaffected by the sulfite liberated through dissociation. Using the kinetics of decomposition of $Hg(SO_3)_2^{2-}$, we have re-evaluated the sequential binding constants for sulfite to the mercuric ion and find a value for K_1 that is four orders of magnitude greater than K_2, which differs from previous estimates in which they were similar in magnitude.

The new values greatly alter speciation predictions for atmospheric Hg in global models. Rather than the major mercury species in clouds being stable $Hg(SO_3)_2^2$, we predict that $HgSO_3$ should predominate in both unpolluted and polluted (by SO_2) air. At 25°C and pH 3, $HgSO_3$ decomposes to Hg^0 in 5 minutes. If this is in fact the major reduction route for mercury, as has been proposed, very little mercury should be present in rainwater. We find evidence for the existence of a highly soluble $Hg^0 \cdot SO_2$ complex. According to our results, the presence of sulfite causes the solubility of Hg(0) to increase by at least three orders of magnitude due to its formation of an SO_2 adduct. This has serious implications for atmospheric deposition, since it may be that the major mercury species in precipitation is the elemental form.

Acknowledgements

First, I would like to thank Dr. Susannah Scott for her advice and support while working on this project. Thanks go also to Elizabeth Mader, who helped perform some of the early experiments. Finally, thanks go to the other members of Dr. Scott's research group for their support.

Table of Contents

Chapter 3. Stabilization of the Aqueous Mercuric Ion by Sulfite

Chapter 4. General Conclusions

Chapter 5. Experimental

List of Figures

Chapter 4

List of Tables

Chapter 2

Chapter 3

Chapter 1

General Introduction

Mercury is classified as a hazardous pollutant by Environment Canada. In recent years, it has been the object of intense regulatory activity. The International Protocol on Heavy Metals requires that emissions of mercury, lead, and cadmium be reduced below 1990 levels. In Canada, the Toxic Substances Management Policy will likely recommend a reduction in environmental mercury emissions to naturally occurring levels. Several bilateral agreements between Canada and the United States exist. In June 1998, the Conference of New England Governors and Eastern Canadian Premiers adopted the Mercury Action Plan which formalizes their commitment to reduce mercury emissions in the region by 50% by 2003 and includes initiatives to improve mercury emission inventories, to monitor and model atmospheric deposition, and plans to monitor the mercury levels in fish and wildlife indicators. Phase II of the North American Regional Action Plan on Mercury, released in August 1999, provides initiatives to deal with the problem of global mercury pollution, primarily through the reduction of mercury emissions.

Mercury has become a topic of such concern due to the appearance of methylmercury contamination in fish.[1] Through bioaccumulation, fish in some lakes now contain mercury at levels which pose a real risk to human health. Mercury enters aquatic systems in a variety of ways: it can be washed in with soil runoff, emitted directly as a component of industrial waste effluent, or deposited from the atmosphere. Ice core samples from Antarctica[2] and peat core samples, whose only mercury sources were the atmosphere,[3] provide records of pre-industrial mercury levels, which are estimated to be 25% of current atmospheric levels.[4] There are now 6000 tons of mercury in the atmosphere,[5] and recent studies suggest that the global concentration is increasing at the rate of 0.6% per

year.[6] High levels of mercury in remote areas, including the Canadian Arctic, suggest that atmospheric deposition is very important.

1.1 The global mercury cycle

Mercury is unique among the metallic elements in that it is the only metal which is a liquid at STP and exists naturally in vapour form, $Hg^0_{(g)}$. However, most mercury is trapped in involatile solids. There are more than twenty-five mercury-containing minerals in the Earth's crust. Cinnabar, HgS, is its primary mineral form, with major deposits in Spain, Slovenia, and Italy.[7]

Natural emissions (from the ocean, soil, volcanoes, and biomass decomposition) are estimated to be responsible for only 40% of the mercury present in the atmosphere today, Figure 1.1. Ocean emissions are considered the most important, however, researchers consider some fraction to be recycled anthropogenic mercury as a result of the 'Grasshopper Effect', in which mercury is revolatilized following its initial deposition. The primary anthropogenic sources are coal burning, waste incineration, and ore roasting, processing, and refining, which together are believed to be responsible for more than 90% of human emissions.[8] Once emitted, natural and human mercury are hard to distinguish, making it difficult to accurately judge the relative contributions of natural and anthropogenic sources. The ocean receives 90% of its mercury through wet and dry deposition[6] from the atmosphere, however the relative importance of each pathway is not known.

Hg concentrations in air and in precipitation have been monitored in an attempt to understand spatial and temporal deposition patterns.[1,4,8,9] For example, in Michigan, wet deposition was greater by a factor of two in the southern sites relative to the northern sites in the state.[7] Similarly, in the Nordic countries, the annual average mercury concentration at the southern site was 15% higher than the central or northern sites.[7]

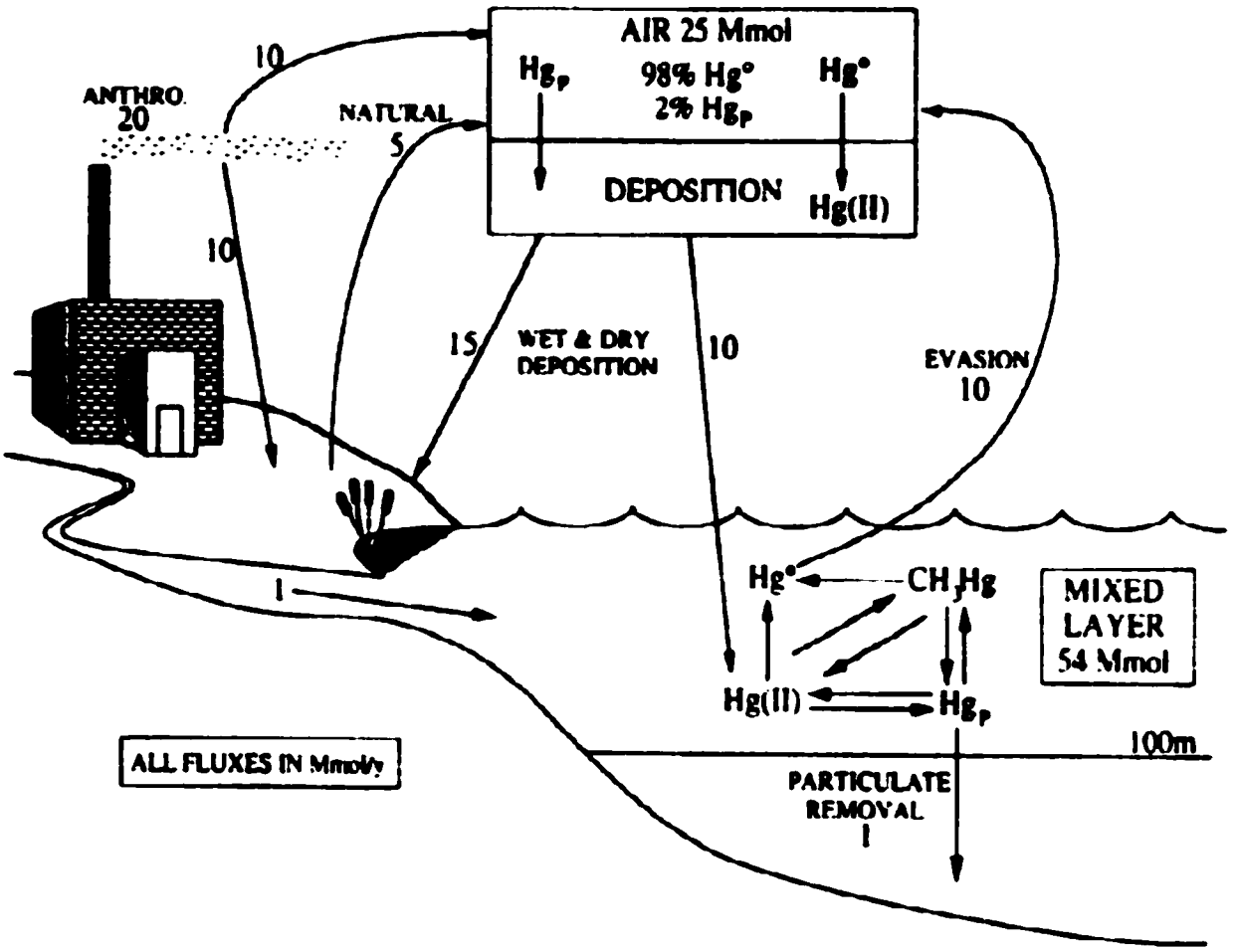

Figure 1.1. The global mercury cycle (after Morel).[6]

Some particulate mercury is directly deposited from the atmosphere. However, more than 98% of all atmospheric mercury is present as Hg^0, which has an estimated lifetime of one year. Conventional wisdom holds that this is not the form in which mercury is deposited; instead, it is first transformed into the more water-soluble form, Hg^{2+}. If this is true, then oxidation processes are important in determining deposition rates. $Hg^{2+}_{(aq)}$ present in clouds may also undergo reduction, after which it may return to the gas phase and be re-subjected to long-range transport.

1.2 The chemistry of mercury

Elemental mercury is unreactive, except in the presence of strong oxidizing agents such as nitric acid. It is fairly insoluble in water with a solubility limit of 3.03×10^{-7} mol/kg H_2O at 298 K.[10] There are two common oxidized forms of mercury. The mercurous ion exists as a dimer, Hg_2^{2+}, which can be formed either by reduction of the mercuric ion or by mixing Hg(II) with Hg^0. Hg_2^{2+} forms compounds with weakly coordinating anions such as sulfate, chlorate, bromate, iodate, and acetate. Oxygen-donor ligands which do not form strong complexes with Hg(II) will also form stable complexes of Hg_2^{2+}, for example, oxalate, succinate, and pyrophosphate.

The presence of strongly coordinating ligands causes Hg_2^{2+} to disproportionate to Hg^0 and Hg(II), eq 1.1.

$$Hg_2^{2+} \leftrightarrows Hg^0 + Hg^{2+} \qquad (1.1)$$

Hg^{2+} binds strongly to soft anions containing S, Cl, Br, and I donor atoms, with which it exhibits a preference for forming linear, 2-coordinate compounds. In the absence of such anions, Hg^{2+} exists as a hexacoordinate aqua complex, $Hg(H_2O)_6^{2+}$, in acidic solutions.

1.3 Atmospheric oxidation of mercury

The concentration of mercury in precipitation is in the range of 1 to 50 ng L^{-1}.[11] Since these values are several orders of magnitude higher than predicted by Henry's law for Hg^0,[12] it is widely believed that more water-soluble forms such as Hg^{2+} are present; oxidation therefore precedes mercury deposition. While a few species in the atmosphere undergo direct photooxidation, this is not the case for Hg^0 since only solar radiation with wavelengths greater than 290 nm can penetrate the lower atmosphere.

Atmospheric oxidation can be mediated by photochemical oxidants. Of the possible oxidants in the atmosphere that may react with Hg^0, the most often-cited is ozone, whose reaction with mercury has been the subject of several studies.[11,13-16] Ozone exists as a trace gas in the troposphere and in the stratosphere. At the Earth's surface, ozone is an important constituent of smog. Its lifetime in summer is five days to a few weeks, whereas in winter it can be greater than three months.[17] Typical background concentrations of ozone are 20 - 30 ppb up to several hundred ppb in heavily polluted air.

The rate of aqueous oxidation of elemental mercury by ozone was estimated[15] from its competition with the known rate of reaction between HSO_3^- and O_3, which has $k = 1 \times 10^6$ M^{-1} s^{-1} at pH 4. Unfortunately, the ozone concentration was not known, but the study concluded that the rate constant for reaction between ozone and mercury must be greater than 1×10^7 M^{-1} s^{-1}. Although this reaction is rapid, very little ozone exists in clouds and, as already noted, Hg^0 is poorly soluble in aqueous solutions.[10] Thus it may be that oxidation by ozone occurs in the gas phase, eq 1.2.

$$Hg^0_{(g)} + O_{3(g)} \rightarrow HgO_{(g)} + O_2 \qquad (1.2)$$

This reaction was studied in a Teflon reaction vessel, where 99% conversion of Hg^0 to Hg^{II} was observed.[11] However, since both Hg^0 and O_3 were adsorbed onto the walls of the reaction vessel, it is possible that the reaction occurred on these

surfaces. While the reaction was found to be first-order with respect to mercury, the order was found to be only 0.81 with respect to ozone. This result may indicate the presence of a heterogeneous reaction, or may be an artefact of the measurements. However, if the oxidation is truly not quite first-order, the expected lifetime of atmospheric mercury is predicted to be only 62 days, which is much shorter than the conventional estimate of one year.

Other potential oxidants for mercury have been studied.[12,16,18-20] In the gas phase, oxidation of Hg^0 by H_2O_2 has been observed.[16] At 20° – 23°C, a rate constant of 5.6×10^{-19} cm^3 $molecule^{-1}$ s^{-1} was calculated. While there is a large uncertainty associated with the calculated value, it is three orders of magnitude smaller than an earlier value,[21] and yields a residence time for mercury of 3.7 – 1.5 years, at an average H_2O_2 concentration of 1 ppb.[16] Therefore the gas phase reaction with peroxide cannot be the only removal process. The aqueous oxidation of Hg^0 by H_2O_2 has also been proposed. [12]

In the marine boundary layer and in polar clouds, oxidation of mercury by reactive chlorine species such as Cl_2 and HOCl may be important.[19] Total concentrations of reactive chlorine species are typically 9 – 254 pptv and vary with altitude. Depending on pH, aqueous chlorine exists as HOCl or as OCl^-, both of which are powerful oxidants. The reaction of HOCl with Hg^0 was proposed as

$$HOCl + Hg^0 \rightarrow Hg^{2+} + Cl^- + OH^- \qquad (1.3)$$

A chemical kinetic model evaluated the importance of oxidation by reactive chlorine species[19] compared to O_3 and ·OH. Above pH 5, oxidation by chlorine species becomes important as the solubility of gaseous chlorine increases. Below pH 3.5, reactive chlorine may not contribute to the oxidation of Hg^0 due to the escape of chlorine from the aqueous phase.

Finally, one avenue that has not been considered for atmospheric mercury reactions is oxidation by other metals. Although most atmospheric mercury exists in the gas phase, other metals are found adsorbed onto particulate matter.

Mercury can be directly oxidized by metal cations in the aqueous phase, as is shown by the oxidation of Hg(I) by Tl(III):[20]

$$Hg_2^{2+} \leftrightarrows Hg^{2+} + Hg^0 \quad (1.4)$$

$$Hg^0 + Tl^{III} \rightarrow Hg^{II} + Tl^{I} \quad (1.5)$$

1.4 The sulfur cycle

Global sulfur emissions to the atmosphere are estimated at (130-180) x 10^{12} g of S per year, of which 15-72 Tg S per year are thought to be natural.[22] Many different sulfur compounds are released into the atmosphere from natural sources such as volcanoes, sea spray, and biological processes. OCS, CS_2, H_2S, and $(CH_3)_2S$ are the most abundant. Except for OCS, these compounds are rapidly oxidized, primarily by $OH^{\cdot}$, to SO_2. SO_2 is a minor component of natural sulfur emissions (from volcanoes) and in clean, continental regions the lower atmosphere has a SO_2 concentration in the range of 70 – 120 pptv.[22]

SO_2 is the primary sulfur compound released through combustion processes. Coal may contain as much as 2-5 wt% S, as organosulfur compounds. The S concentration in crude oil is 1-2 wt%. However, during oil refining, sulfur compounds are retained in the heavy residues so that the lighter oils are relatively clean. Natural gas may contain some H_2S but it is removed prior to transportation because it is corrosive to the containers. During combustion of fossil fuels, reduced sulfur is oxidized to SO_2 and released. Globally, approximately 60% of all fossil sulfur emissions come from coal combustion while 30% are from oil and refined product combustion, for a total estimated emission of 70 Tg S per year. [22] In Western Europe, 45% of all emitted sulfur dioxide is from the generation of electricity while another 40% is released by the industrial sector (75% of which is from fuel combustion).[23] Polluted continental areas have atmospheric concentrations of up to 10^4 pptv SO_2.[22]

The oxidation of SO_2 to S(VI) occurs mainly in clouds, with a typical lifetime of two days. SO_2 is quite soluble in water. Like CO_2, it is hydrated, eq 1.6.[23]

$$SO_{2(aq)} + H_2O \leftrightarrows SO_2{\cdot}H_2O \qquad K_H = 1.23\ M\ atm^{-1} \qquad (1.6)$$

Unlike $CO_2{\cdot}H_2O$, $SO_2{\cdot}H_2O$ does not rearrange to form H_2SO_3. Recent calculations[25] confirm that the formation of H_2SO_3 is unfavourable. However, the aicd-base behaviour of SO_2 solutions is analogous to that of carbonic acid, eq 1.7–1.8:[24]

$$SO_2{\cdot}H_2O \leftrightarrows HSO_3^- + H^+ \qquad K_{a1} = 0.024\ M \qquad (1.7)$$

$$HSO_3^- \leftrightarrows SO_3^{2-} + H^+ \qquad K_{a2} = 1.62 \times 10^{-7}\ M \qquad (1.8)$$

The first acid dissociation yields two tautomers, in which the proton is either bound to S, to give bisulfite, HSO_3^-, or to O, resulting in hydrosulfate, $SO_2(OH)^-$. The major isomer is thought to be bisulfite.[26]

1.5 Reduction of sulfite by metal ions

Sulfite may coordinate to metal centres as either a S or an O donor in either a monodentate or bidentate manner, as shown in complexes I to IV.

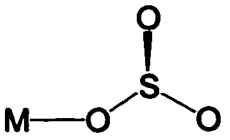

I

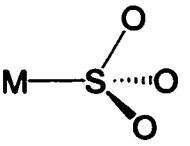

II

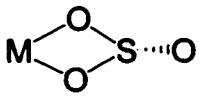

III

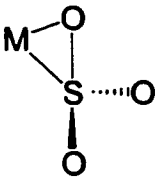

IV

These bonding modes have been identified using Raman and infrared spectroscopy.[27,28] Many metal-sulfite complexes are quite stable and have been crystallized for identification, for example, $(NH_4)_2[Hg(SO_3)_2]$.[30]

Other transition metal-sulfite complexes undergo redox decomposition. The mode of coordination, through S or O, can affect the rate of reduction. For example, O-bonded $Co(NH_3)_5SO_3$ undergoes intramolecular redox approximately 100 times faster than the S-bonded complex.[29] In some cases, sulfite may initially bind through oxygen and then isomerize to a sulfur-bonded complex, as is the case for *cis*-$[Pt(NH_3)_4(OH_2)(OSO_2)]^{2+}$ which rearranges to *cis*-$[Pt(NH_3)_4(OH_2)(SO_3)]^{2+}$ before Pt(IV) undergoes reduction. [30]

Sulfite reacts with oxoanions by oxygen atom abstraction to form sulfate directly, as is the case for ferrate:[31]

$$HSO_3^- + FeO_4^{2-} \leftrightarrows [O_3Fe^{VI}\text{-}O\text{-}SO_3H]^{3-} \quad (1.9)$$

$$[O_3Fe^{VI}\text{-}O\text{-}SO_3H]^{3-} \rightarrow Fe^{IV} + SO_4^{2-} \quad (1.10)$$

Other transition metals undergo one-electron transfer reactions. Sulfite may undergo single-electron transfer to form the sulfite radical anion, which dimerizes to dithionate, $S_2O_6^{2-}$, or two-electron oxidation to sulfate. Inner-sphere reactions produce $S_2O_6^{2-}$ as the final product, with a reaction stoichiometry of one metal ion per S(IV).[32] Mn(III) is proposed to undergo inner-sphere reduction.[33]

$$2\ MnOH^{2+} + 2\ HSO_3^- \rightarrow 2\ Mn^{2+} + S_2O_6^{2-} + 2\ H_2O \quad (1.11)$$

Outer-sphere one-electron transfers result in formation of a S(VI) product and have a reaction stoichiometry of two metals per S(IV), as is the case for Os(III):[32]

$$[Os^{III}(bpy)_3]^{3+} + SO_3^{2-} \leftrightarrows [Os^{II}(bpy)_3]^{2+} + SO_3^{-\bullet} \quad (1.12)$$

$$[Os^{III}(bpy)_3]^{3+} + SO_3^{-\bullet} \rightarrow [Os^{II}(bpy)_3]^{2+} + SO_3 \quad (1.13)$$

$$SO_3 + H_2O \leftrightarrows SO_4^{2-} + H^+ \quad (1.14)$$

Inner-sphere two-electron transfers may occur via halide abstraction. Such is the case for reduction of Au(III) halides by sulfite:[34]

$$[Au^{III}Y_2X_2]^- + SO_3^{2-} \rightarrow [Au^{I}Y_2]^- + X^- + XSO_3^- \qquad X = Cl^-, Br^- \quad (1.15)$$

$$XSO_3^- + H_2O \rightarrow HSO_4^- + X^- + H^+ \quad (1.16)$$

Metals such as Pt^{IV} undergo inner-sphere two-electron redox with SO_3^{2-} to give M^{n+2} and S(VI): [30]

$$Pt^{IV}(NH_3)_4(SO_3)(SO_3H)^+ + H_2O \rightarrow Pt^{II}(NH_3)_3(SO_3) + NH_4^+ + HSO_4^- + H^+ \quad (1.17)$$

Chapter 2

Reduction of the Aqueous Mercuric Ion by Sulfite

2.1 Introduction

The rate of reduction of mercuric ions by excess HSO_3^- was the subject of a previous report, in which the observed rate law was deemed valid only under conditions where the predominant species is $Hg(SO_3)_2^{2-}$ [35] since solutions containing equimolar amounts of Hg^{2+} and sulfite at room temperature decompose to Hg^0 and sulfate within minutes at room temperature. $HgSO_3$ has been reported to be unstable[36] and was not directly observed. The rate of its decomposition was estimated from a composite rate constant, assuming $HgSO_3$ to be a steady-state intermediate in the decomposition of $Hg(SO_3)_2^{2-}$.

In this chapter, we report a reinvestigation of the reduction of the aqueous mercuric ion by sulfite in acidic solution. We have observed the $HgSO_3$ complex under conditions where it is formed quantitatively and directly measured the rate constant for its decomposition, avoiding several of the assumptions made in previous work.

2.2 Results

2.2.1 Formation and UV spectrum of $HgSO_3$

We discovered that $HgSO_3$ can readily be observed by UV-visible spectroscopy provided the reactant solutions are chilled to at least 15°C prior to mixing. A spectrum was recorded immediately following addition of 40 μM sulfite to an air-saturated solution of 400 μM Hg^{2+} in 1 mM $HClO_4$ at 15°C. A peak was

observed with λ_{max} = 234 nm, Figure 2.1a. Its intensity varies linearly with the concentration of added sulfite in the range 8 - 67 μM, Figure 2.2, yielding the extinction coefficient ϵ(234 nm) = (1.57 ± 0.05) x 10^4 M^{-1} cm^{-1}. The spectrum is virtually invariant with pH; in 0.1 M $HClO_4$, ϵ(234 nm) = (1.63 ± 0.07) x 10^4 M^{-1} cm^{-1}. We propose that the absorbing species is unprotonated $HgSO_3$, as in eq 2.1.

$$Hg^{2+}_{(aq)} + HSO_3^-{}_{(aq)} \leftrightarrows HgSO_{3(aq)} + H^+_{(aq)} \qquad (2.1)$$

2.2.2 Stoichiometry of $HgSO_3$ decomposition

The initial spectrum of the $HgSO_3$ solution changes with time. This process is shown in Figure 2.3 for a solution containing 37 μM $HgSO_3$ and 400 μM Hg^{2+} at pH 3 and 15.0 °C. There are two clean isosbestic points at 219 and 224 nm. The final spectrum is identical to that of independently prepared Hg_2^{2+}, with peaks at 236, 215, and 204 nm, Figure 2.1b. The yield of Hg_2^{2+} depends linearly upon the initial concentration of $HgSO_3$. The apparent extinction coefficient of the peak at 236 nm is ϵ = (2.74 ± 0.09) x 10^4 M^{-1} cm^{-1} based on the initial concentration of $HgSO_3$, Figure 2.4. For comparison, the reported spectrum of $Hg_2^{2+}{}_{(aq)}$ has ϵ(236 nm) = 2.8 x 10^4 M^{-1} cm^{-1}.[37,38] The reaction stoichiometry established by this result is shown in eq 2.2.

$$HgSO_3 + Hg^{2+} + H_2O \rightarrow Hg_2^{2+} + HSO_4^- + H^+ \qquad (2.2)$$

The yield of Hg_2^{2+} was identical in a reaction performed in the absence of dissolved oxygen.

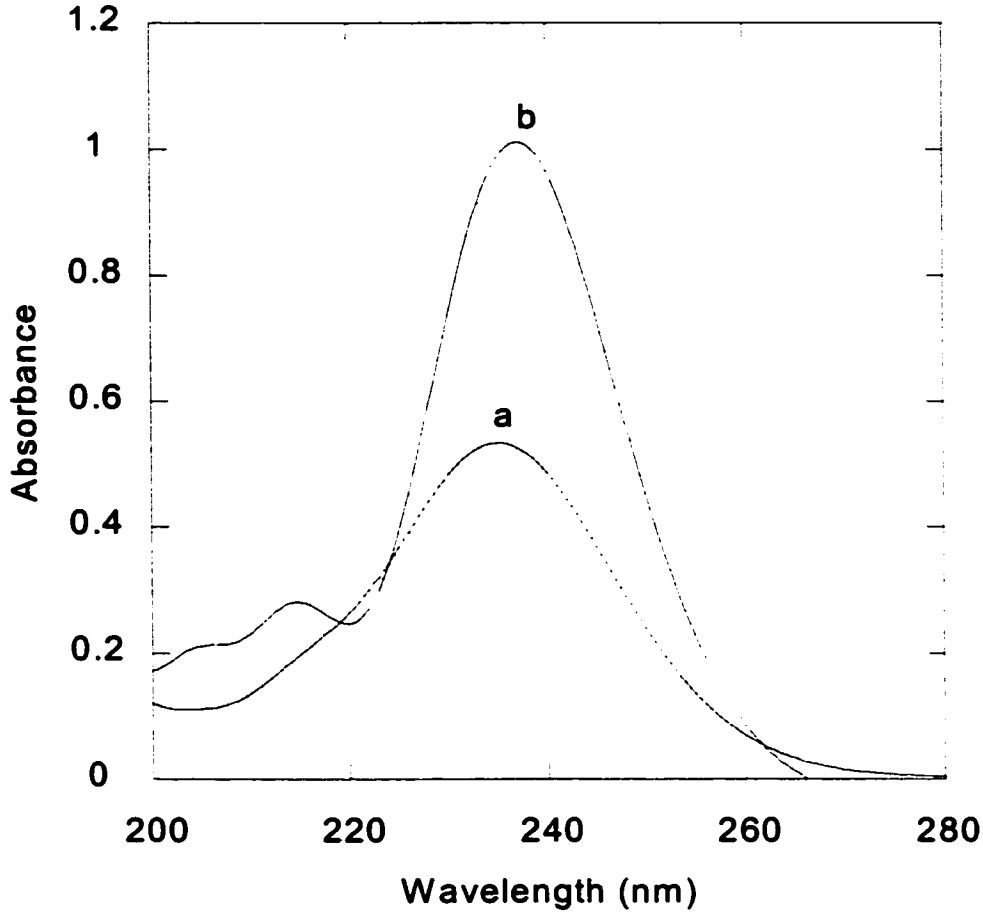

Figure 2.1. UV spectra of (a) 40 μM $HgSO_3$, and (b) 40 μM Hg_2^{2+}, at pH 3 ($HClO_4$).

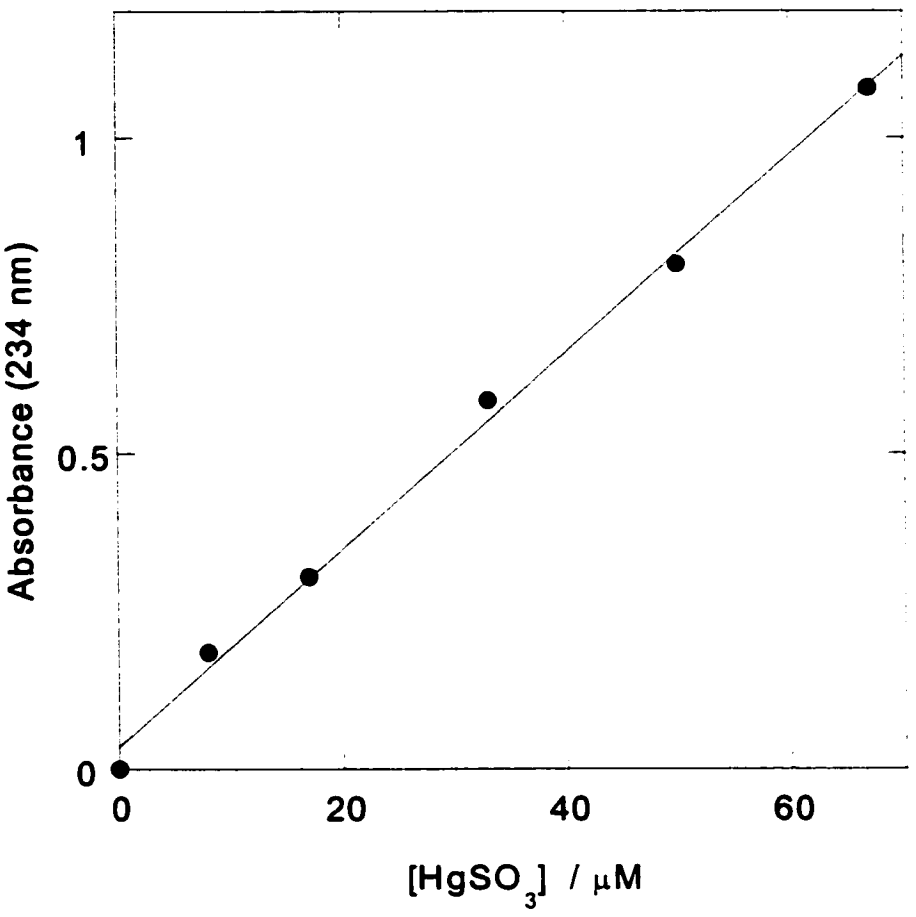

Figure 2.2. Extinction coefficient determination for $HgSO_3$ at pH 3 ($HClO_4$).

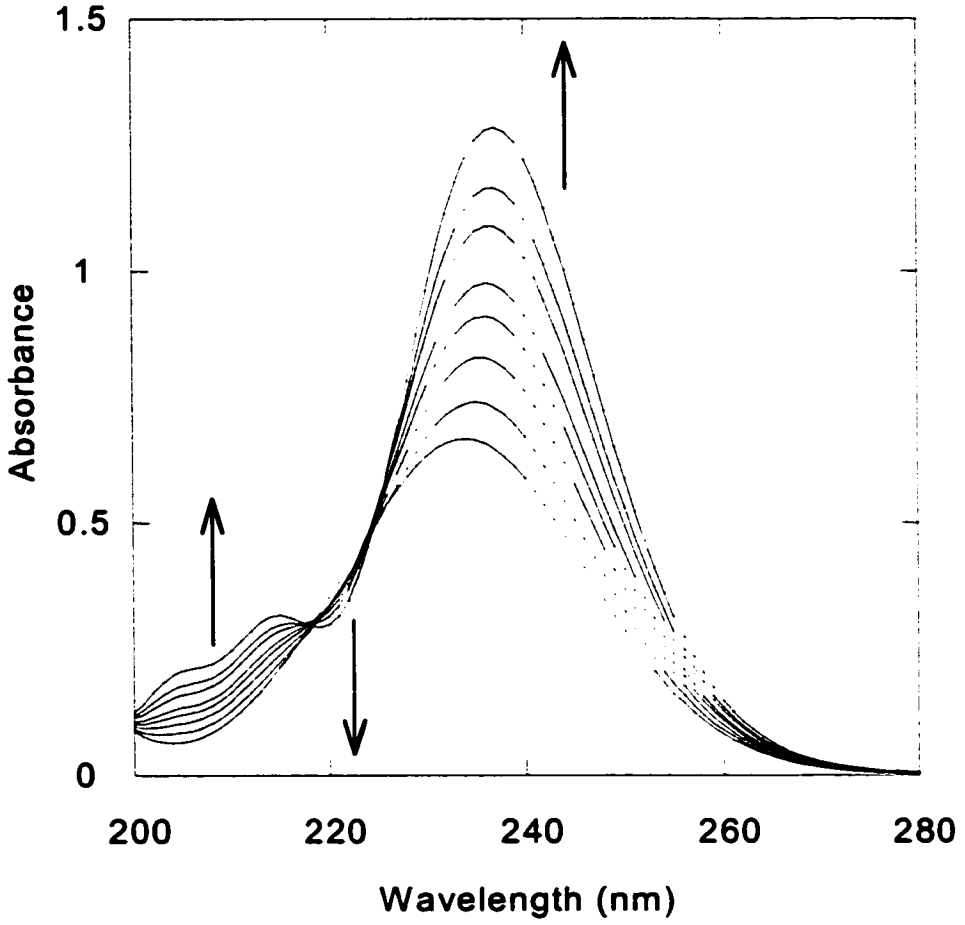

Figure 2.3. Evolution of the spectrum of 37 μM $HgSO_3$ in the presence of 400 μM Hg^{2+}, over the course of 15 min at 15.0°C and at pH 3 ($HClO_4$).

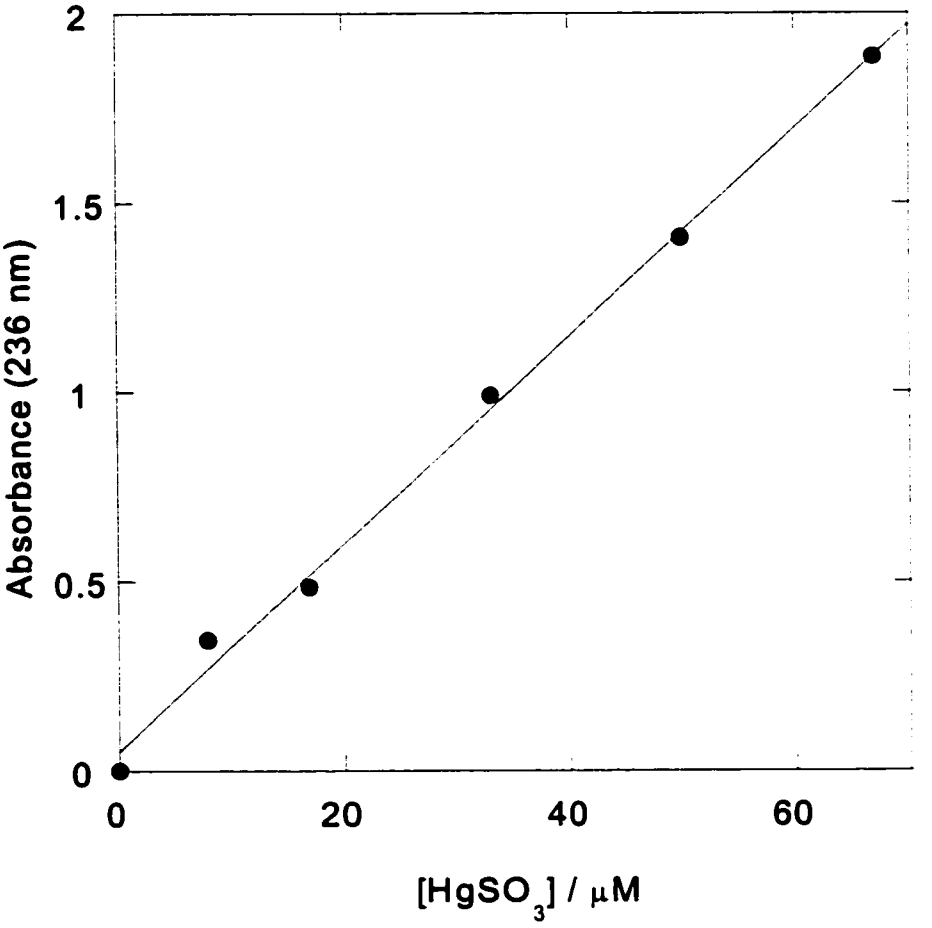

Figure 2.4. Extinction coefficient determination of the product of decomposition of $HgSO_3$.

3.1.3 Rate Law

The kinetics of the reaction were followed by monitoring the increase in absorbance at 236 nm, where $\Delta\varepsilon = 1.2 \times 10^4\ M^{-1}\ cm^{-1}$. The time-evolution of the absorbance change is accurately described by a single exponential function, characteristic of a first-order reaction. The first-order rate constant is independent of [$HgSO_3$] and free [Hg^{2+}] (present in excess) and insensitive to the presence or absence of [$O_{2(aq)}$], Figure 2.5. The rate constant is invariant with ionic strength in the range 0.001 to 1.0 M ($HClO_4/NaClO_4$), Figure 2.6. Thus the rate law is authentically first-order and not pseudo-first-order (except for the kinetically undetectable participation of water). The measured rate constants are collected in Table 2.1.

These results are consistent with rate-determining intramolecular reduction of the mercuric ion within the $HgSO_3$ complex, eq 2.3, followed by rapid comproportionation of $Hg^0_{(aq)}$ with free Hg^{2+}, eq 2.4.

$$HgSO_{3(aq)} \rightarrow Hg^0_{(aq)} + S(VI) \qquad (2.3)$$

$$Hg^{2+}_{(aq)} + Hg^0_{(aq)} \leftrightarrows Hg_2^{2+}{}_{(aq)} \qquad (2.4)$$

The rate constant for comproportionation is $5.9 \times 10^8\ M^{-1}\ s^{-1}$ and the equilibrium constant is $1.8 \times 10^8\ M^{-1}$ at 25°C,[10] therefore the formation of Hg_2^{2+} is fast and quantitative (as demonstrated by the curve fits in Figures 2.4 and 2.5). Note that this value of the equilibrium constant is valid for dissolved $Hg^0_{(aq)}$, not $Hg_{(l)}$. Since comproportionation is rapid, Hg^0 never accumulates and therefore its concentration does not exceed its solubility in water. The lack of a significant ionic strength effect on the rate reflects the absence of charge separation in the rate-determining step. The indifference of the rate to the presence of dissolved oxygen requires that radical intermediates such as $SO_3^{\bullet-}$ are not involved. The rate law at pH 3 is therefore

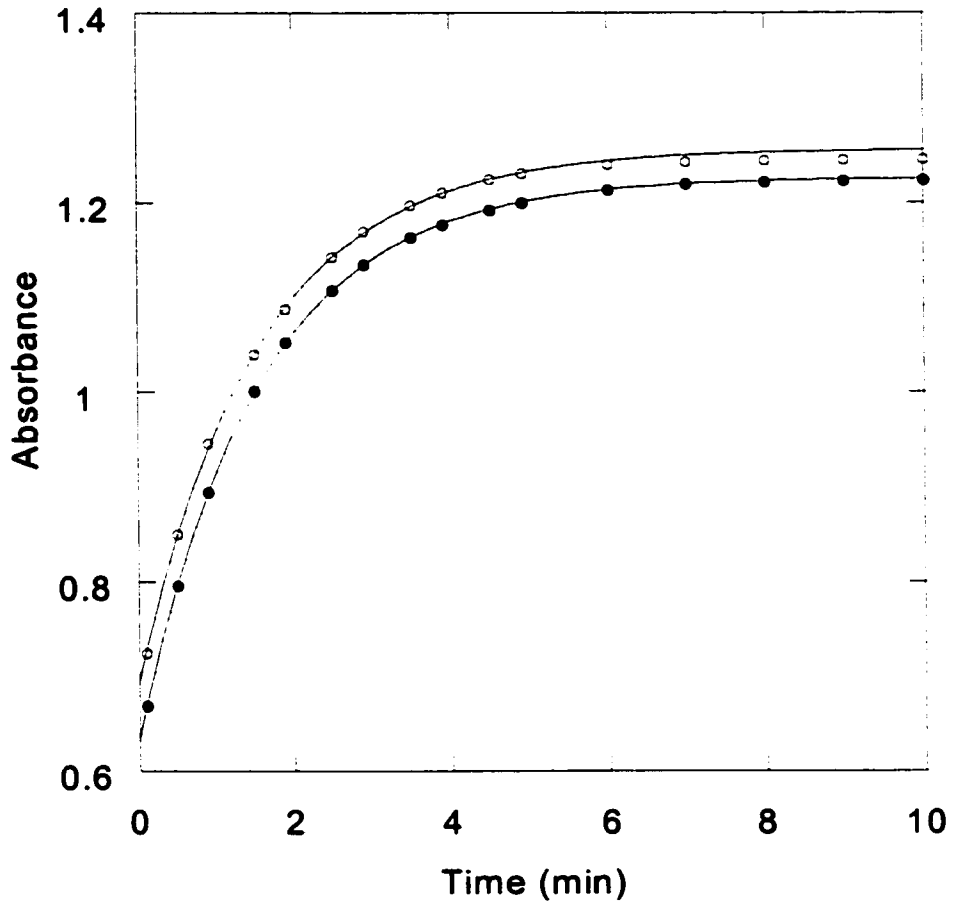

Figure 2.5. Kinetic profiles for decomposition of $HgSO_3$ in the presence of excess Hg^{2+} at 25.0°C and pH 3 ($HClO_4$); open circles: air-saturated, closed circles: argon-saturated solution. The latter were slightly offset to better display the data.

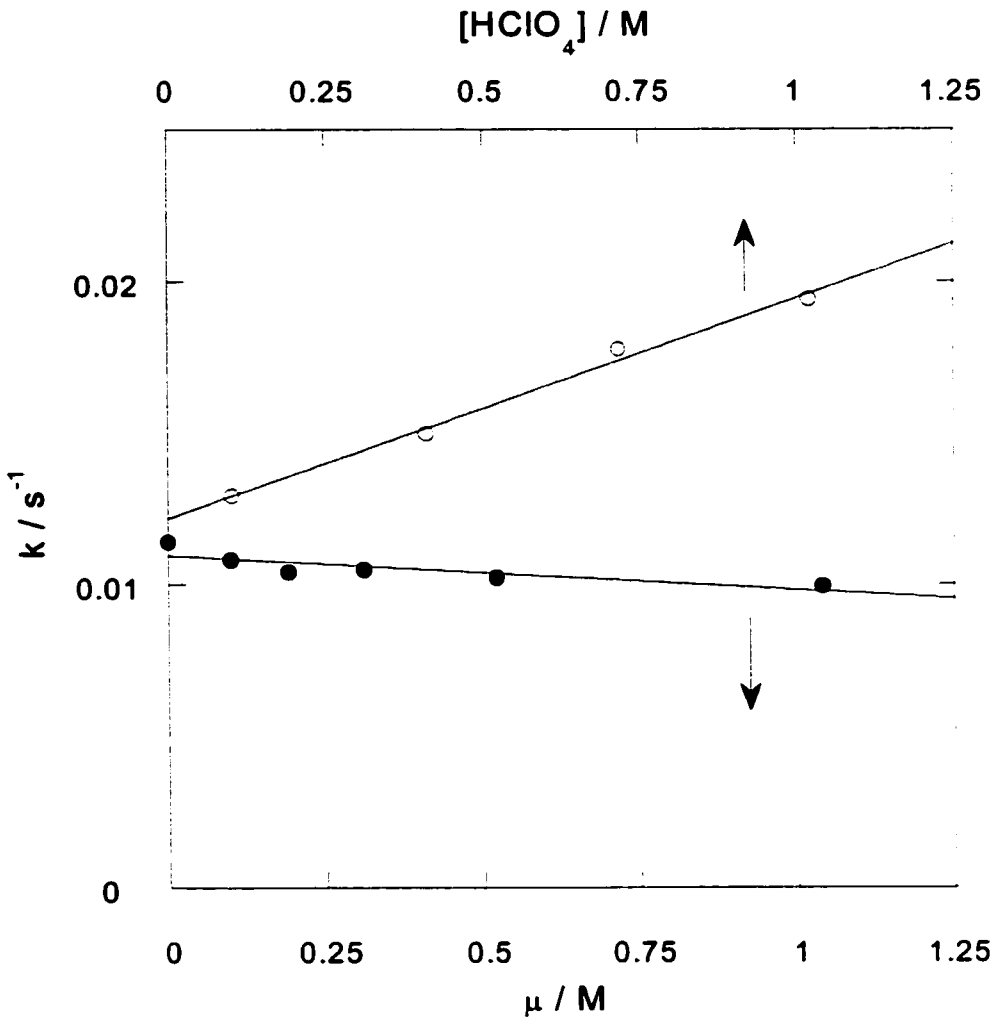

Figure 2.6. Dependence of the first-order rate constants for $HgSO_3$ decomposition on ionic strength ($HClO_4/NaClO_4$) at pH 3 (closed circles), and acid ($HClO_4$) at ionic strength μ =1.08 M ($HClO_4/NaClO_4$) (open circles).

Table 2.1. Rate constants for intramolecular reduction of mercuric ion by sulfite at 25.0°C

$[Hg^{2+}]$ mM	[S(IV)] [a] mM	$[HClO_4]$ M	$[NaClO_4]$ M	10^3 k [b] s^{-1}	$[Hg^{2+}]$ mM	[S(IV)] [a] mM	$[HClO_4]$ M	$[NaClO_4]$ M	10^3 k [b] s^{-1}
0.400	0.040	0.001		10.75 ± 0.07	0.333	0.029	0.100		12.60 ± 0.05
0.400	0.040	0.001		10.770 ± 0.001[c]	0.333	0.009	0.100		12.7 ± 0.3 (3)
0.333	0.010	0.003		10.9 ± 0.1	0.333	0.018	0.100		13.2 ± 0.2 (3)
0.333	0.010	0.003		10.4 ± 0.1	0.333	0.042	0.100		12.7 ± 0.5 (2)
0.333	0.029	0.003		11.18 ± 0.03	0.830	0.042	0.100		13.3 ± 0.5 (3)
0.333	0.030	0.003		9.138 ± 0.007	0.650	0.011	0.100		12.40 ± 0.02
0.333	0.009	0.003		11.7 ± 0.5 (3)	0.333	0.010	0.100		13.2 ± 0.7 (2)[c]
0.400	0.040	0.004		12.468 ± 0.003	0.333	0.010	0.100		12.8 ± 0.5 [d]
0.400	0.040	0.006		12.680 ± 0.005	0.333	0.055	0.100		12.48 ± 0.02
0.400	0.040	0.008		12.83 ± 0.01	0.333	0.092	0.100		12.3 ± 0.2
0.333	0.030	0.003	0.100	9.082 ± 0.005	0.333	0.009	0.100	0.050	13.0 ± 0.5 (2)
0.333	0.009	0.003	0.100	10.8 ± 0.3 (4)	0.333	0.030	0.100	0.0910	11.8 ± 0.1
0.333	0.010	0.003	0.100	9.0 ± 0.2	0.333	0.032	0.100	0.310	12.5 ± 0.1
0.333	0.010	0.003	0.180	8.8 ± 0.3	0.333	0.032	0.100	0.520	11.95 ± 0.02
0.333	0.030	0.003	0.191	10.40 ± 0.07	0.333	0.034	0.100	1.000	11.57 ± 0.07 (2)

a Total added sulfite, i.e., sum of $[SO_3^{2-}]$, $[HSO_3^-]$, and $[SO_{2(aq)}]$.

b Number of experiments is shown in parentheses, where greater than one. Errors are standard deviations of the average rate constant, except for single experiments, where the error in the non-linear least squares fit is shown.

c Argon-saturated. In all other experiments, the solutions were air-saturated.

d Hg^{2+} was the last reagent added. In all other experiments, sulfite was the last reagent added.

$$-d[HgSO_3]/dt = d[Hg_2^{2+}]/dt = k_0 [HgSO_3] \quad (2.5)$$

The rate constant at (25.0 ± 0.2) °C, pH 3 and ionic strength μ = 0.0026 M is k_0 = (0.0106 ± 0.0009) s^{-1}.

2.2.4 Acid dependence

Although the UV spectrum of $HgSO_3$ is unaffected by lowering the pH from 3 to 1 (*vide supra*), the rate constant for its decomposition is slightly higher at the lower pH. The effect is linear in $[H^+]$ at constant ionic strength μ = 1.08 M, Figure 2.6, with slope (0.0084 ± 0.0006) M^{-1} s^{-1}. The complete expression for the first-order rate constant in this pH range is therefore

$$k = k_0 + k_1[H^+] \quad (2.6)$$

where k_0 = (0.0113 ± 0.0003) s^{-1} and k_1 = (0.0084 ± 0.0006) M^{-1} s^{-1}. At pH 3, the acid-catalyzed path contributes less than 0.1% to the overall rate of decomposition, such that $k \approx k_0$. The stoichiometry at pH 0 is the same as that shown in eq 2.2, *i.e.*, one Hg_2^{2+} is formed per $HgSO_3$.

2.2.5 Temperature effect

The rate of decomposition of $HgSO_3$ is strongly temperature-dependent. Rate constants at temperatures ranging from 5 - 35 °C are shown in Table 2.2. Each 10° increase in temperature results in roughly a quadrupling of the rate constant. At pH 3, the Eyring plot, Figure 2.7, is linear with slope (–1.26 ± 0.04) x

Table 2.2. Temperature dependence of the rate constants for reduction of mercuric ion by sulfite.

pH	Temperature °C	k s^{-1}	Number of Expts
3	6.5	0.00055 ± 0.00005	2
3	15.5	0.0027 ± 0.0001	2
3	25.0	0.0106 ± 0.0009	15
3	35.0	0.040 ± 0.002	2
1	6.6	0.000675 ± 0.000015	3
1	16.0	0.00303 ± 0.00005	4
1	25.0	0.0129 ± 0.0003	17
1	34.4	0.048 ± 0.012	5

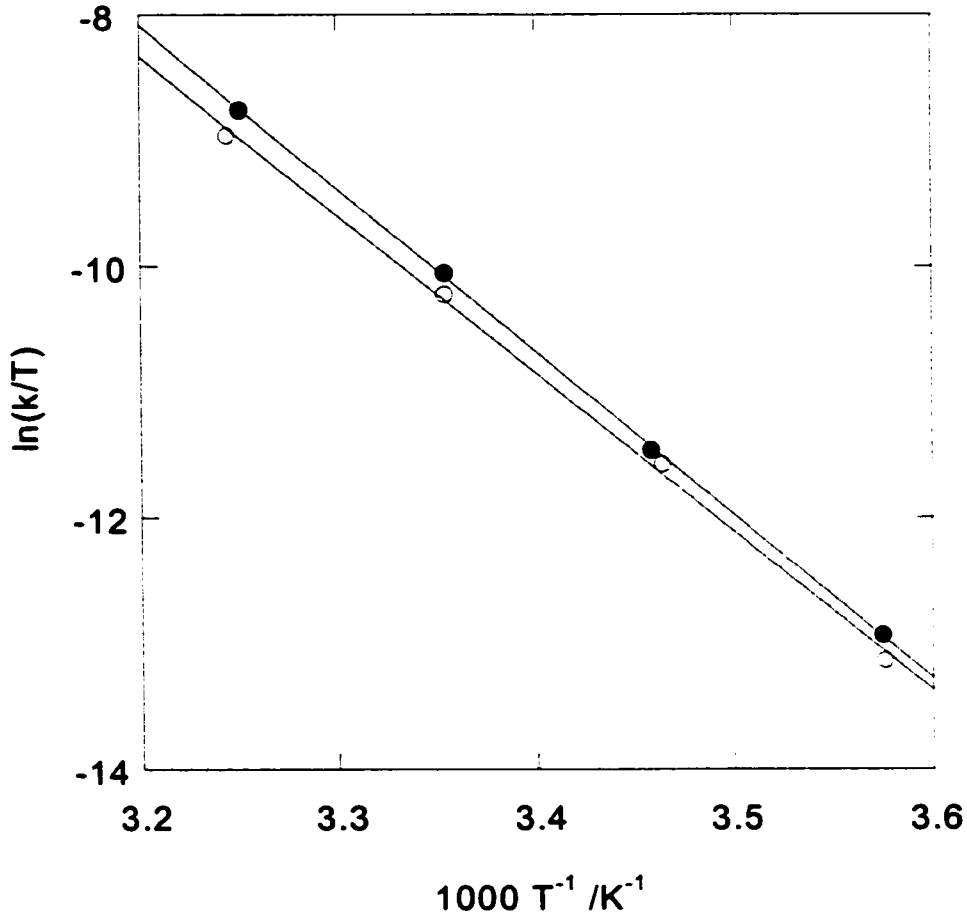

Figure 2.7. Eyring plot of the temperature-dependent rate constants for $HgSO_3$ decomposition. Open circles: pH 3; closed circles: pH 1.

10^4 K and intercept (32 ± 1). Since the reaction is elementary, the form of the Eyring equation is:

$$\ln(k/T) = \ln(R/Nh) + \Delta S^{\ddagger}/R - \Delta H^{\ddagger}/RT \qquad (2.7)$$

The values derived for $\Delta H^{\ddagger}$ and $\Delta S^{\ddagger}$ are (105 ± 2) kJ/mol and (68 ± 6) J/mol·K, respectively.[39] The errors were derived from the appropriate error propagation formulae:[40]

$$\left(\sigma\Delta H^{\ddagger}\right)^2 = \frac{R^2 T_{max}^2 T_{min}^2}{\Delta T^2}\left\{\left(\frac{\sigma T}{T}\right)^2\left[\left(1+T_{min}\frac{\Delta L}{\Delta T}\right)^2+\left(1+T_{max}\frac{\Delta L}{\Delta T}\right)^2\right]+2\left(\frac{\sigma k}{k}\right)^2\right\} \qquad (2.8)$$

$$\left(\sigma\Delta S^{\ddagger}\right)^2 = \frac{R^2}{\Delta T^2}\left\{\left(\frac{\sigma T}{T}\right)^2\left[T_{max}^2\left(1+T_{min}\frac{\Delta L}{\Delta T}\right)^2+T_{min}^2\left(1+T_{max}\frac{\Delta L}{\Delta T}\right)^2\right]+\left(\frac{\sigma k}{k}\right)^2\left(T_{max}^2+T_{min}^2\right)\right\} \qquad (2.9)$$

where $\Delta T = (T_{max} - T_{min})$ and $\Delta L = \left[\ln\left(\frac{k_{max}}{T_{max}}\right) - \ln\left(\frac{k_{min}}{T_{min}}\right)\right]$

The comparable Eyring plot at pH 1 is almost parallel, Figure 2.7, with $\Delta H^{\ddagger}$ = (108 ± 1) kJ/mol and $\Delta S^{\ddagger}$ = (81 ± 5) J/mol·K.

3.2 Discussion

2.3.1 The nature of $HgSO_3$

Although aqueous sulfite exists almost exclusively as HSO_3^- at pH 3, its complex with the mercuric ion, $HgSO_3$, is not protonated. Its UV spectrum is acid-independent, and its rate of decomposition at pH 3 is almost independent of ionic strength, as expected for a neutral complex whose reaction involves little or no charge formation in the transition state. The intense band at 234 nm in the UV spectrum of $HgSO_3$ is consistent with ligand-to-metal charge transfer in a sulfur-bonded sulfito complex.[29] For comparison, the spectrum of $Pt(NH_3)_3(SO_3)$ consists of a peak at 234 nm with ϵ = 5650 M^{-1} cm^{-1}.[30] The reported IR spectrum of the more stable $Hg(SO_3)_2^{2-}$ complex confirms metal-sulfur coordination.[27,28]

Thus $HgSO_3H^+$ is spectroscopically undetectable in our experiments, although it makes a significant contribution to the rate of decomposition in strongly acidic solution. The first-order $[H^+]$-dependence in eq 2.6 requires that a proton be present in the transition state for the acid-catalyzed path. Since protonation equilibria for oxyanions are usually established very quickly and are therefore unlikely to be rate determining, the most probable origin of the second term in eq 2.6 is the presence of the $HgSO_3H^+$ complex, eq 2.10.

$$HgSO_3H^+ \leftrightarrows HgSO_3 + H^+ \qquad (2.10)$$

A substantial increase in pK_a occurs for Bronsted acid ligands upon coordination to a Lewis acidic metal cation. For example, the pK_a of $HgCO_3H^+$ is 4.1,[41] compared to 10.3 for CO_3H^-. Since SO_3H^- (est. pK_a 5.4)[42] is a considerably stronger acid than CO_3H^-, the pK_a of $HgSO_3H^+$ is predicted to be < 1. The relative contribution of $HgSO_3H^+$ to the overall rate of decomposition is 7% at pH 1 and 43% at pH 0. $HgSO_3H^+$ can be kinetically significant although spectroscopically

unobservable provided its rate constant is much higher than the rate constant k_0 for decomposition of the major species $HgSO_3$.

2.3.2 Mechanism of the redox reaction

The redox decomposition of $HgSO_3/HgSO_3H^+$ amounts to the reduction of the mercuric ion to Hg^0 by coordinated sulfite. When free $Hg^{2+}_{(aq)}$ is present, its trapping of the Hg^0 product to give the strongly absorbing Hg_2^{2+} ion serves as a convenient kinetic probe for the reaction. The observation of two isosbestic points in the evolution of the spectrum of $HgSO_3$ to that of Hg_2^{2+} is consistent with a reaction that has no observable intermediates. The decomposition of $HgSO_3$ is an authentic first-order reaction, confirming that the redox reaction is intramolecular, as previously suggested.[35] However, our rate constant for decomposition of $HgSO_3$ is about 50 times slower than previously reported. In that study, a composite rate constant was measured in the presence of excess sulfite, and the value of the equilibrium constant for sulfite dissociation from $Hg(SO_3)_2^{2-}$ was estimated in order to obtain an approximate value for k_0. By choosing conditions under which the rate law is particularly simple, as in eq 2.5, we have instead measured the value of k directly.

Our kinetic results also require a reevaluation of the previously proposed mechanism.[35] The intramolecular redox reaction generates neither Hg^+ nor sulfite radical anions. The latter are rapidly trapped by dissolved oxygen, which initiates a chain autoxidation of sulfite,[43] eq 2.11 – 2.13.

$$SO_3^{\cdot-} + O_2 \rightarrow SO_5^{\cdot-} \quad (2.11)$$

$$SO_5^{\cdot-} + SO_3^{2-} \rightarrow SO_4^{\cdot-} + SO_4^{2-} \quad (2.12)$$

$$SO_4^{\cdot-} + SO_3^{2-} \rightarrow SO_4^{2-} + SO_3^{\cdot-} \quad (2.13)$$

Since we found that the stoichiometry of the reduction of mercuric ion by sulfite, as well as its rate constant, are independent of the concentration of

dissolved oxygen, we can rule out one-electron transfer mechanisms with radical intermediates. The observed Hg_2^{2+} product must therefore be formed by comproportionation of Hg^0 with Hg^{2+} rather than by dimerization of Hg^+.

Our direct measurement of k_0 also permits a straightforward evaluation of its temperature dependence. Global mercury models assume that this reaction is temperature-independent,[44] based on a published remark that temperature effects in this system are small.[35] We find that the rate constant k_0 roughly quadruples with each 10°C increase in temperature. The activation parameters are very large and positive. Both their signs and magnitudes are consistent with a unimolecular reaction involving significant bond-breaking in the transition state. However, the magnitude of the entropy value suggests that while the mechanism involves the participation of water molecules, they must coordinate prior to the bond cleavage.

Sulfite is known to reduce various metal ions by one-electron transfer[23,45] (for example, MnO_4^-),[46] by oxygen atom abstraction (for example, ferrate),[31] and by halide abstraction (for example, $AuCl_4^-$).[34] The redox decomposition of $HgSO_3$ does not appear to belong to any of these categories. It most resembles the intramolecular acid-catalyzed reduction of Pt(IV) in *cis*-$Pt(NH_3)_4(SO_3)_2$ to $Pt(NH_3)_3(SO_3)$.[30]

Concerted two-electron transfer may be accomplished by heterolytic cleavage of the metal-sulfur bond. $HgSO_3$, although formed as a mercuric-sulfite complex, is formally equivalent to a donor-acceptor adduct of mercury(0) with sulfur trioxide. In other words, while the sulfite anion brought both electrons of the Hg-S bond into its union, it leaves them behind when it departs, eq 2.14.

$$Hg^{2+}_{(aq)} + SO_3^{2-}{}_{(aq)} \leftrightarrows Hg^{II}S^{IV}O_3 \rightarrow Hg^0S^{VI}O_3 \rightarrow Hg^0_{(aq)} + S(VI) \quad (2.14)$$

Both SO_3 and SO_2 are known to be capable of forming strong donor-acceptor complexes with Lewis bases such as NH_3 and transition metals such as Ni(0).[47-49]

The hydration of SO_3 by H_2O has been studied kinetically in the gas phase,[50] and a donor-acceptor complex, **V**, has been characterized by microwave spectroscopy.[51] Its conversion to H_2SO_4 requires a second water molecule, **VI**, to form a structure in which S-O bond formation and proton migration are concerted within the six-membered ring.[52,53]

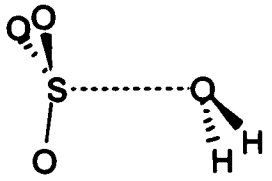

V

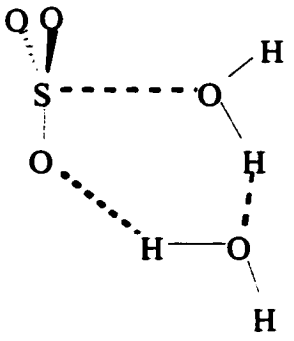

VI

We propose that a similar water-assisted departure of the sulfite ligand as either $SO_3 \cdot H_2O$ or $H_2SO_4 \cdot H_2O$ may induce the redox decomposition of $HgSO_3$. The mercury coordination number in $HgSO_3$ is not known, but there is likely at least one water molecule in its primary coordination sphere, and it is probably subject to strong trans-labilization by the sulfite ligand.[29] The transition state for the redox reaction must incorporate an additional one or two water molecules in the second coordination sphere, **VII** and **VIII**.

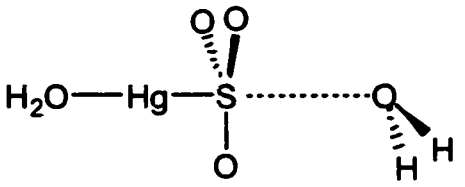

VII

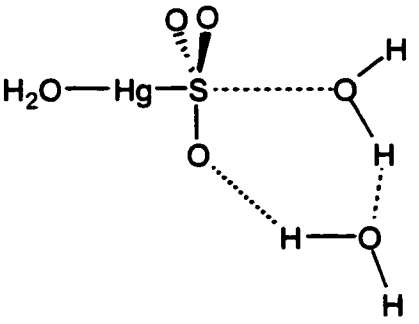

VIII

Protonation of the sulfite ligand, as in $HgSO_3H^+$, will make the donor-acceptor interaction with H_2O stronger and obviate the need for proton transfer from the second water molecule, thus accelerating the reaction.

This mechanism for sulfite reduction of Hg^{2+} can, when coupled with the rapid reoxidation of $Hg^0_{(aq)}$ by dissolved O_3,[54] also be viewed as a mercury-catalyzed path for the oxidation of S(IV) to S(VI).

2.4 *Conclusion*

Aqueous hydrogen sulfite reacts with Hg^{2+} to form, in the absence of excess HSO_3^-, the $HgSO_3$ complex, observed here for the first time. Its UV spectrum is described by ϵ (234 nm) = (1.57 ± 0.05) x 10^4 M^{-1} cm^{-1}. $HgSO_3$ decomposes in an intramolecular redox reaction which is kinetically first-order. The rate constant is independent of $[Hg^{2+}]$, $[HSO_3^-]$, $[O_{2(aq)}]$ and ionic strength. An acid-assisted pathway becomes significant at pH ≤ 1, attributed to the contribution of $HgSO_3H^+$. The rate of the intramolecular reaction of $HgSO_3$ was measured by trapping the Hg^0 product as Hg_2^{2+}; the value of the rate constant is k_0 = (0.0106 ± 0.0009) s^{-1} at 25.0°C, pH 3. The activation parameters for pH 3, $\Delta H^{\ddagger}$ and $\Delta S^{\ddagger}$, are (105 ± 2) kJ/mol and (68 ± 6) J/mol·K, respectively, consistent with a unimolecular bond cleavage mechanism. A pathway involving H_2O-induced concerted $2e^-$ transfer is proposed.

Chapter 3

Stabilization of the Aqueous Mercuric Ion by Sulfite

3.1 Introduction

$HgSO_3$ is not generally assumed to be the dominant atmospheric mercuric species when the ambient S(IV) concentration greatly exceeds $[Hg]_{total}$, as is the case even in clean air. Under natural conditions, it has been suggested that $Hg(SO_3)_2^{2-}$ is a major mercury species present in atmospheric water droplets.[35]

$$Hg^{2+}_{(aq)} + SO_3^{2-}{}_{(aq)} \leftrightarrows HgSO_{3(aq)} \qquad K_1 \qquad (3.1)$$

$$HgSO_{3(aq)} + SO_3^{2-}{}_{(aq)} \leftrightarrows Hg(SO_3)_2^{2-}{}_{(aq)} \qquad K_2 \qquad (3.2)$$

Unfortunately, the sequential formation constants for mercuric-sulfite complexes, eq 3.1-3.2, are not measurable by conventional methods because of the short lifetime of $HgSO_{3(aq)}$.[36] The overall formation constant, eq 3.3, is known since $Hg(SO_3)_2^{2-}$ is considerably more stable than $HgSO_3$, particularly in neutral or alkaline solutions.

$$Hg^{2+}_{(aq)} + 2\,SO_3^{2-}{}_{(aq)} \leftrightarrows Hg(SO_3)_2^{2-}{}_{(aq)} \qquad \beta_2 \qquad (3.3)$$

Since reduction of the mercuric ion appears to proceed uniquely via the $HgSO_3$ complex, the magnitudes of the sequential formation constants are important parameters for models of the global mercury cycle.

In this chapter, a kinetic study of the reduction of the mercuric ion in aqueous solution in the presence of excess S(IV) is described. In combination with results from the previous chapter, the formation constants for mercuric-sulfite complexes can be extracted from kinetic measurements. Evidence is

further presented that the product of the redox reaction may not be, as previously supposed, $Hg^0_{(aq)}$, but a soluble complex of Hg^0 with SO_2.

3.2 Results

3.2.1 UV spectrum of $Hg(SO_3)_2^{2-}$

The formation of a complex between two sulfite anions and an aqueous mercuric cation, $Hg(SO_3)_2^{2-}{}_{(aq)}$, has been reported in neutral and acidic mercuric ion solutions containing excess uncoordinated HSO_3^-. The UV-visible spectrum in acidic solution (pH 3, $HClO_4$) is reported to consist of a peak at 230 nm with ϵ = 27 000 M^{-1} cm^{-1}.[35] The UV spectrum was recorded following addition of 180 μM sulfite to an air-saturated solution of 40 μM Hg^{2+} in 1.0 mM $HClO_4$. The spectrum of complex **IX** consists of a peak at λ_{max} = 230 nm, Figure 3.1a. Its intensity varies linearly with the concentration of mercuric ion, with ϵ(230 nm) = (2.98 ± 0.01) x 10^4 M^{-1} cm^{-1} after subtraction of the spectral contribution of free HSO_3^-, Figure 3.2a. Upon adjusting the pH of the solution to 12 with NaOH, and after spectral subtraction of the contribution due to the free SO_3^{2-}, a peak was observed with λ_{max} = 215 nm, Figure 3.1b. Its intensity also varies linearly with the concentration of mercuric ion, Figure 3.2b, yielding ϵ(215 nm) = (1.68 ± 0.02) x 10^4 M^{-1} cm^{-1} for complex **X**.

3.2.2 Spectrophotometric titration

The pH-dependence of the UV spectrum was further investigated by titration. The pH of a solution containing 40 μM $Hg(SO_3)_2^{2-}$ and 1.5 mM free SO_3^{2-} initially at pH 13 was gradually lowered to pH 3 by addition of aliquots of $HClO_4$. The absorbance at 230 nm after each addition is shown as a function of

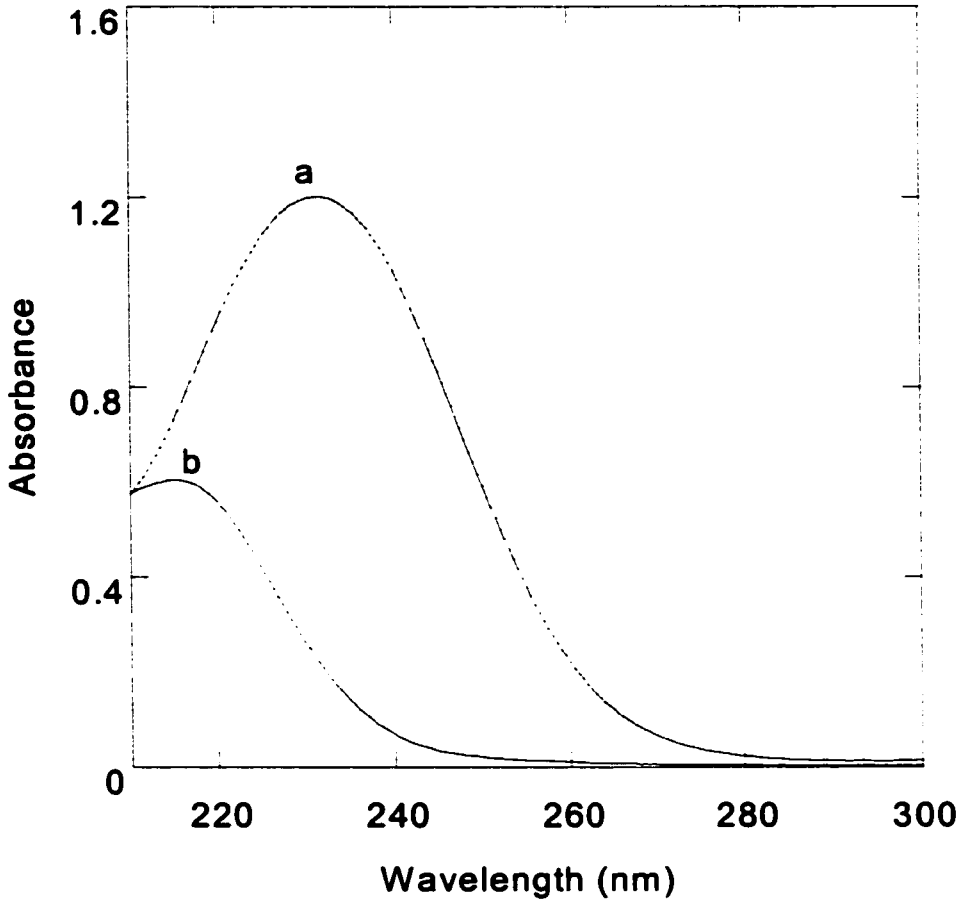

Figure 3.1. UV spectrum of 40 μM $Hg(SO_3)_2^{2-}$ in the presence of 0.10 mM free HSO_3^- at (a) pH 3; and (b) pH 12, in a 1 cm pathlength cell. In each case, the UV spectrum of free HSO_3^- has been subtracted.

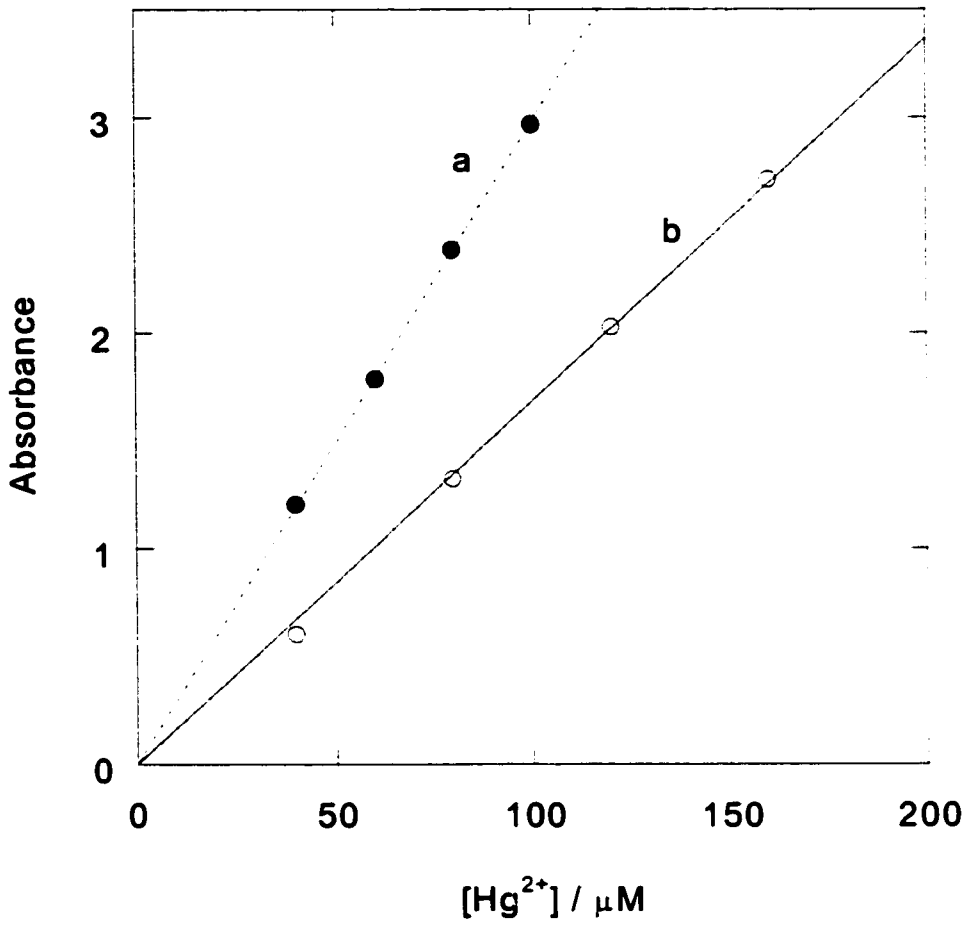

Figure 3.2. Determination of the extinction coefficient of $Hg(SO_3)_2^{2-}$ at (a) pH 3, λ_{max} = 230 nm; and (b) pH 12, λ_{max} = 215 nm.

pH in Figure 3.3. Two K_a values are required to account for the behaviour of the UV spectrum over this pH range. The extinction coefficients of complexes **IX** and **X** were fixed at their measured values, $\epsilon_I = 2.98 \times 10^4$ and $\epsilon_{II} = 7.3 \times 10^3$ M^{-1} cm^{-1}, at 230 nm. The curve in Figure 3.3 was accurately reproduced with a three-parameter fit to eq 3.4:

$$Abs = [Hg^{2+}]_{total} (\epsilon_I [H^+] + \epsilon_{II} K'')/([H^+] + K'') + [S(IV)]_{free} (\epsilon' K')/([H^+] + K') \quad (3.4)$$

in which the first term represents the pH-dependent contribution of mercury-sulfite complexes to the total absorbance and the second term the pH-dependent contribution of SO_3^{2-}. The parameters of the non-linear curve fit are $K' = (1.3 \pm 0.2) \times 10^{-7}$, $K'' = (2.0 \pm 0.2) \times 10^{-12}$ and $\epsilon' = (676 \pm 11)$ M^{-1} cm^{-1}. K' agrees with the known acid dissociation constant for HSO_3^-, $K_{a2} = 1.6 \times 10^{-7}$ at $\mu = 0.1$ M,[24] while ϵ' is reasonably close to our independently measured value for SO_3^{2-} at 230 nm, 525 ± 19 M^{-1} cm^{-1} (the value of ϵ for HSO_3^- at this wavelength is negligible).

We therefore assign K'' to the equilibrium between complexes **IX** and **X**. The protonated form, complex **IX**, is the predominant mercury species in acidic solution, and thus in all the kinetic work that follows. Based on the results described below, we believe complex **IX** corresponds to $Hg(SO_3)_2^{2-}$. Its deprotonation in alkaline solution must therefore involve a coordinated water molecule, eq 3.5:

$$\underset{\textbf{IX}}{Hg(SO_3)_2(H_2O)_n^{2-}} \leftrightarrows \underset{\textbf{X}}{Hg(SO_3)_2(H_2O)_{n-1}(OH)^{3-}} + H^+ \; ; \; K'' = 2.0 \times 10^{-12} \quad (3.5)$$

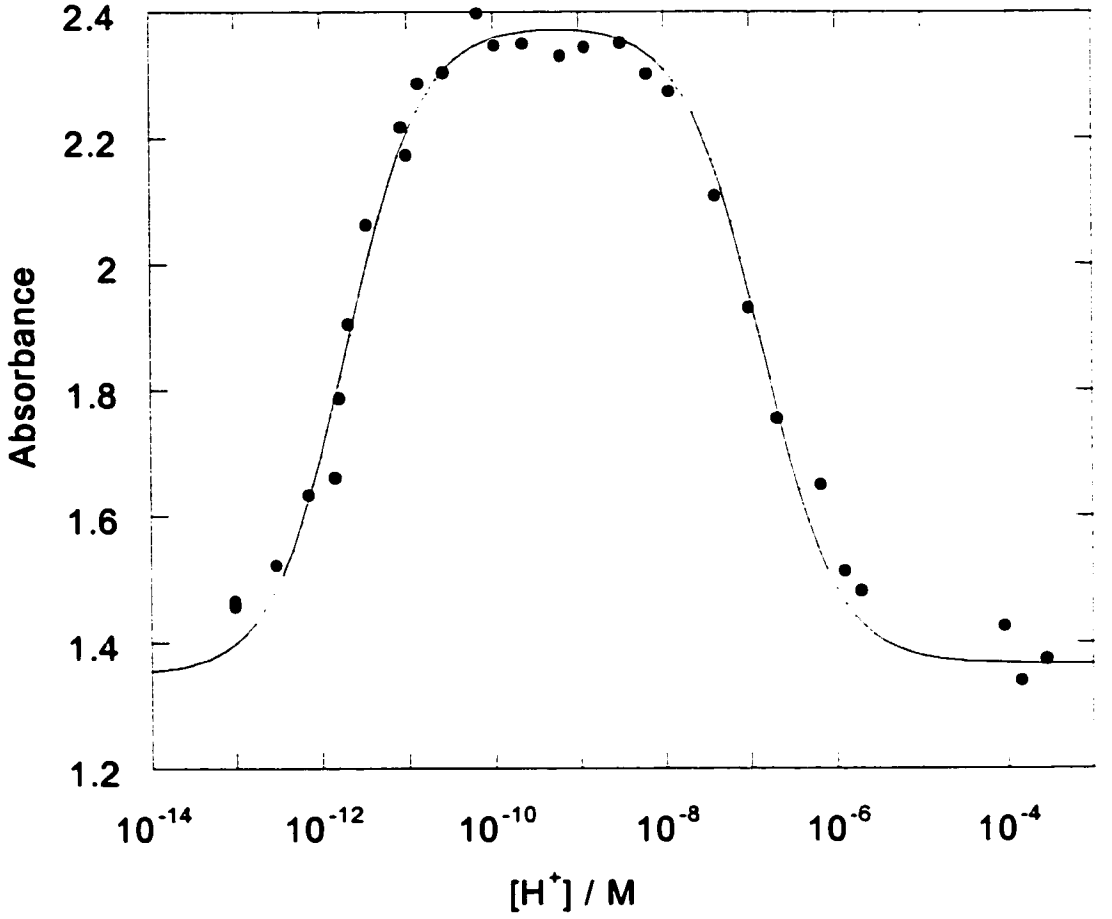

Figure 3.3. Spectrophotometric titration of 40 μM $Hg(SO_3)_2^{2-}$ in the presence of 1.50 mM free HSO_3^-/SO_3^{2-} from pH 13 to pH 4, with $HClO_4$. The solid line is the three-parameter non-linear least-squares fit to eq 3.5.

3.2.3 Rate law for reduction of the mercuric ion

The complex $Hg(SO_3)_2^{2-}$ is not stable indefinitely, although it decomposes more slowly than does $HgSO_3$.[55] Addition of 40 μM Hg^{2+} to a freshly-prepared air-saturated solution containing 150 μM HSO_3^- in 1.0 mM $HClO_4$ at 45°C causes a first-order decay of intensity at 230 nm, Figure 3.4a. An identical curve was obtained when the experiment was repeated with argon-saturated solutions, Figure 3.4b. The rate is thus independent of the presence of dissolved oxygen. It is also independent of the concentration of $Hg(SO_3)_2^{2-}$: experiments in the presence of 81 μM uncoordinated HSO_3^- gave the same pseudo-first-order rate constants for the decay of both 40 μM and 80 μM $Hg(SO_3)_2^{2-}$.

The pseudo-first-order rate constants vary linearly with the concentration of $[H^+]$ at constant $[HSO_3^-]$ = 200 μM, and inversely with the concentration of uncoordinated HSO_3^- at constant pH = 3.0 and μ = 0.10 M ($NaClO_4$). Taken together, these observations imply that the reaction is inhibited by free SO_3^{2-}. Its concentration was calculated from the acid dissociation constants for $SO_{2(aq)}$ and HSO_3^-, K_{a1} = 0.024 and $K_{a2} = 1.6 \times 10^{-7}$.[24] Most rate constants were measured at 45°C, Table 3.1, a temperature at which the decomposition of $Hg(SO_3)_2^{2-}$ is conveniently fast. The plot of k_{obs}^{-1} vs. free $[SO_3^{2-}]$, Figure 3.5, contains both variable $[H^+]$ and variable $[HSO_3^-]$ data. The pseudo-first-order rate constant k_{obs} is therefore described by:

$$k_{obs}^{-1} = a + b\,[SO_3^{2-}] \qquad (3.6)$$

with a = (55 ± 14) s and b = $(1.25 \pm 0.05) \times 10^{10}$ s M^{-1} at 45°C and μ= 0.10 M ($NaClO_4$).

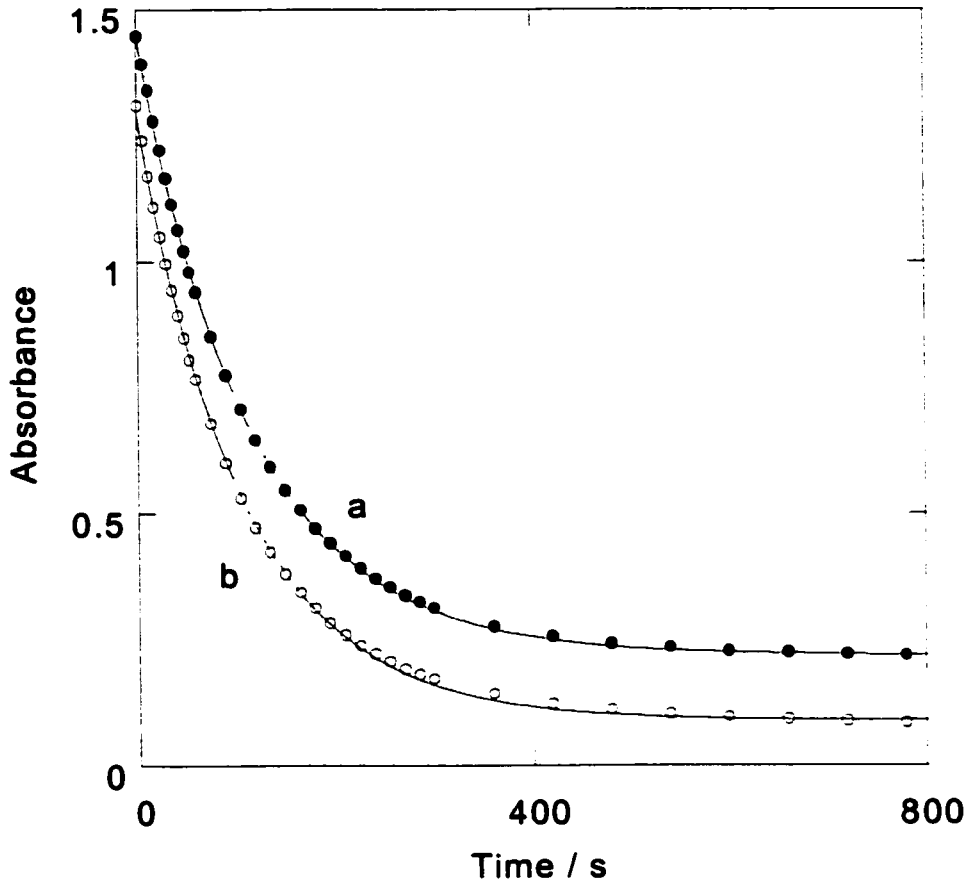

Figure 3.4. Kinetic profiles for the decomposition of 40 μM $Hg(SO_3)_2^{2-}$ at pH 3 and 45°C, in the presence of 0.15 mM free HSO_3^-, in (a) air-saturated; and (b) air-free solutions. The curves are slightly offset to better display the data. Solid lines are non-linear least-squares fits to the integrated first-order rate equation.

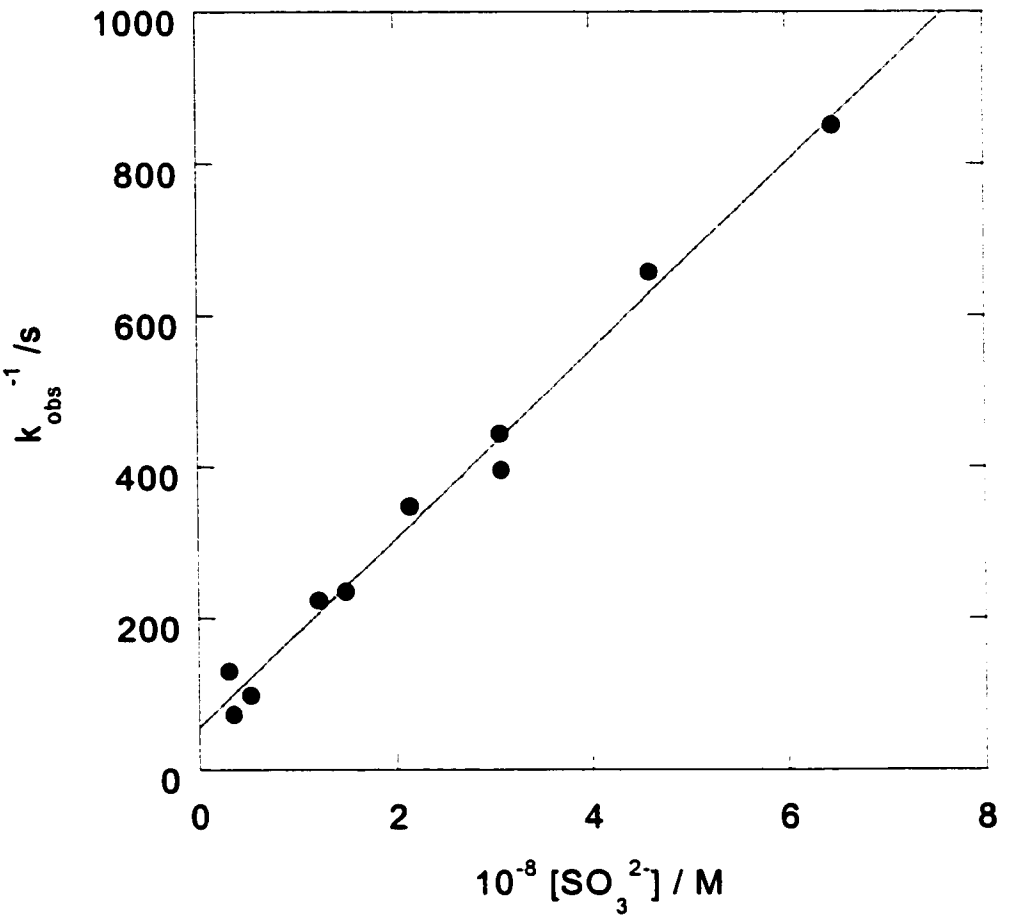

Figure 3.5. Dependence of the inverse of the pseudo-first-order rate constants for decomposition of 40 μM $Hg(SO_3)_2^{2-}$ on the concentration of uncoordinated SO_3^{2-}, at 45°C and μ = 0.10 M ($NaClO_4$).

Table 3.1. Pseudo-first-order rate constants for the redox decomposition of $Hg(SO_3)_2^{2-}$ at μ = 0.10 M ($NaClO_4$).

T / °C	[S(IV)] / mM[a]	[H^+] / mM[b]	10^4 k_{obs} / s^{-1} [c]
25.2	0.077	1.0	1.233 ± 0.007
	0.140	1.0	0.7134 ± 0.003
	0.200	1.0	0.400 ± 0.001
35.5	0.10	1.0	8.0 ± 0.7
	0.20	1.0	4.2 ± 0.3
	0.32	1.0	1.8 ± 0.3
	0.50	1.0	1.25 ± 0.3
45.2	0.020	1.0	77 ± 1
	0.079	1.0	45 ± 1
	0.14	1.0	28.7 ± 0.6
	0.20	1.0	22.6 ± 0.6
	0.30	1.0	15.2 ± 0.9
	0.20	2.0	25.3 ± 0.6
	0.20	5.0	42.5 ± 0.3
	0.20	7.0	102.0 ± 0.3
	0.20	10.0	136.9 ± 0.3
55.0	0.098	1.0	122 ± 3
	0.21	1.0	90.1 ± 0.7
	0.43	1.0	56 ± 1

a Sum of contributions of $SO_{2(aq)}$ and HSO_3^-, not coordinated to mercury.

b In excess of the amount required to protonate the sulfite not coordinated to mercury.

c Errors are from non-linear least squares fit to the integrated first-order rate equation.

3.2.4 Temperature dependence

Similar kinetic behaviour was observed at temperatures between 26 and 55°C, Table 3.2. However, at temperatures below 45°C, the value of a is insignificantly different from zero. The Eyring plot constructed for the kinetic parameter b^{-1}, Figure 3.6, is linear with slope -(2.00 ± 0.05) x 10^4 K^{-1} and intercept (34 ± 1). From these values, we obtain the apparent activation parameters $\Delta H_{obs}^{\ddagger}$ = (166 ± 4) kJ/mol and $\Delta S_{obs}^{\ddagger}$ = (85 ± 11) J/K·mol.

3.2.5 Products

Since non-UV-absorbing products, in particular $S_2O_6^{2-}$, may be generated in sulfite oxidations by metal ions,[23] we determined the quantity of unreacted S(IV) after completion of its reaction with Hg(II). Iodometric titration of a solution originally containing 14.5 μmol $Hg(SO_3)_2^{2-}$ and 28.7 μmol uncoordinated HSO_3^-, following decomposition of the $Hg(SO_3)_2^{2-}$, resulted in an endpoint at 43.2 μmol HSO_3^-. Thus the spent solution contains all of the S(IV) present initially as free $HSO_{3(aq)}^-$ as well as one equiv. of S(IV) released from $Hg(SO_3)_2^{2-}$ as it decomposes to Hg^0. We confirmed independently that $S_2O_6^{2-}$ is not detected by iodometric titration, nor does it react with either $Hg(SO_3)_2^{2-}$ or Hg^{2+}.

The final spectrum of the solution after reduction of the mercuric ion by excess sulfite consists of a broad peak centred at 276 nm, Figure 3.7a. Its apparent ϵ, based on $[Hg]_{total}$, is 94 M^{-1} cm^{-1}. The UV spectrum of $SO_{2(aq)}$ also consists of a peak at 276 nm, with ϵ = 430 M^{-1} cm^{-1}.[56] However, $SO_{2(aq)}$ constitutes only a small fraction of the total S(IV) content of the solution at pH 3 and contributes little to the spectrum, Figure 3.7b. The nature of the species responsible for the peak in the product spectrum is discussed below.

Table 3.2. Temperature dependence of kinetic parameters for the reduction of mercuric ion in the presence of excess aqueous sulfite

T / °C	k_d^{-1} / s	$10^{11} K_2 / k_r$	k_r / s^{-1} [55]
25.2	- [a]	9 ± 2	0.0106
35.5	- [a]	1.2 ± 0.1	0.040
45.2	55 ± 14	0.125 ± 0.005	0.134
55.0	51 ± 3	0.0194 ± 0.0008	0.462

a Insignificantly different from zero, based on the data obtained in Table 3.1.

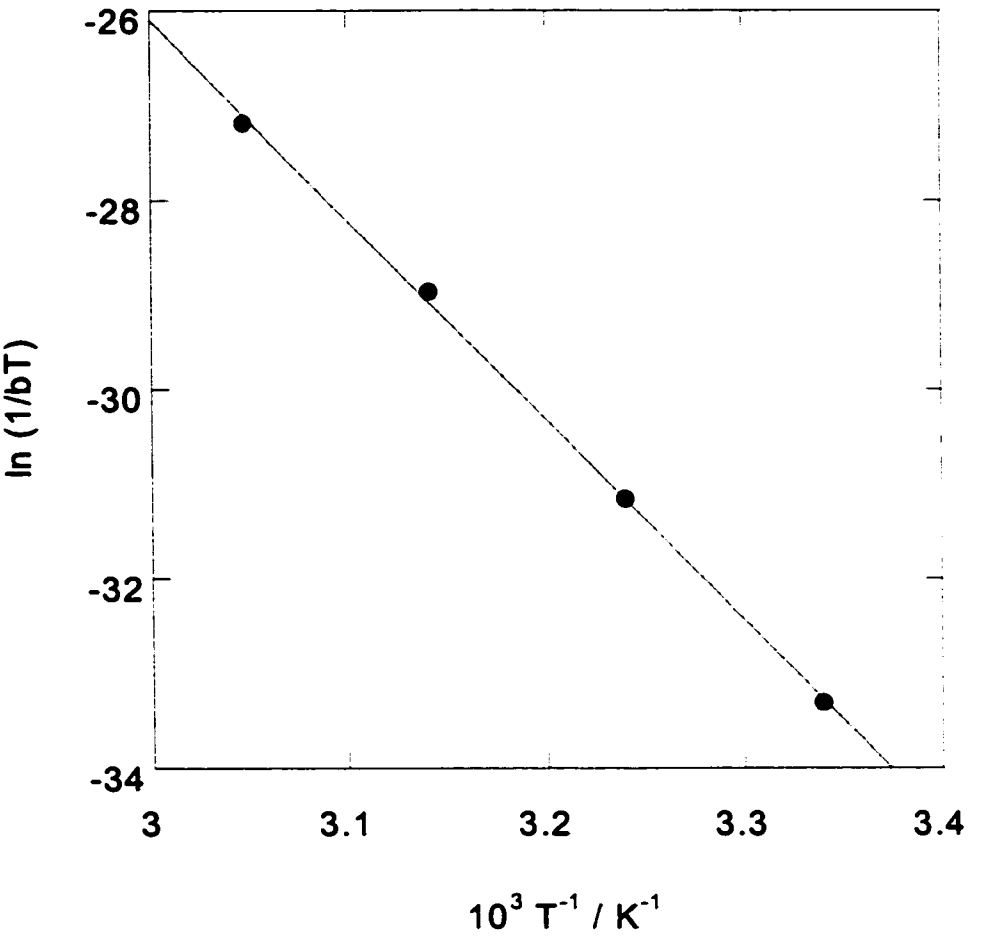

Figure 3.6. Eyring plot for the redox decomposition of $Hg(SO_3)_2^{2-}$.

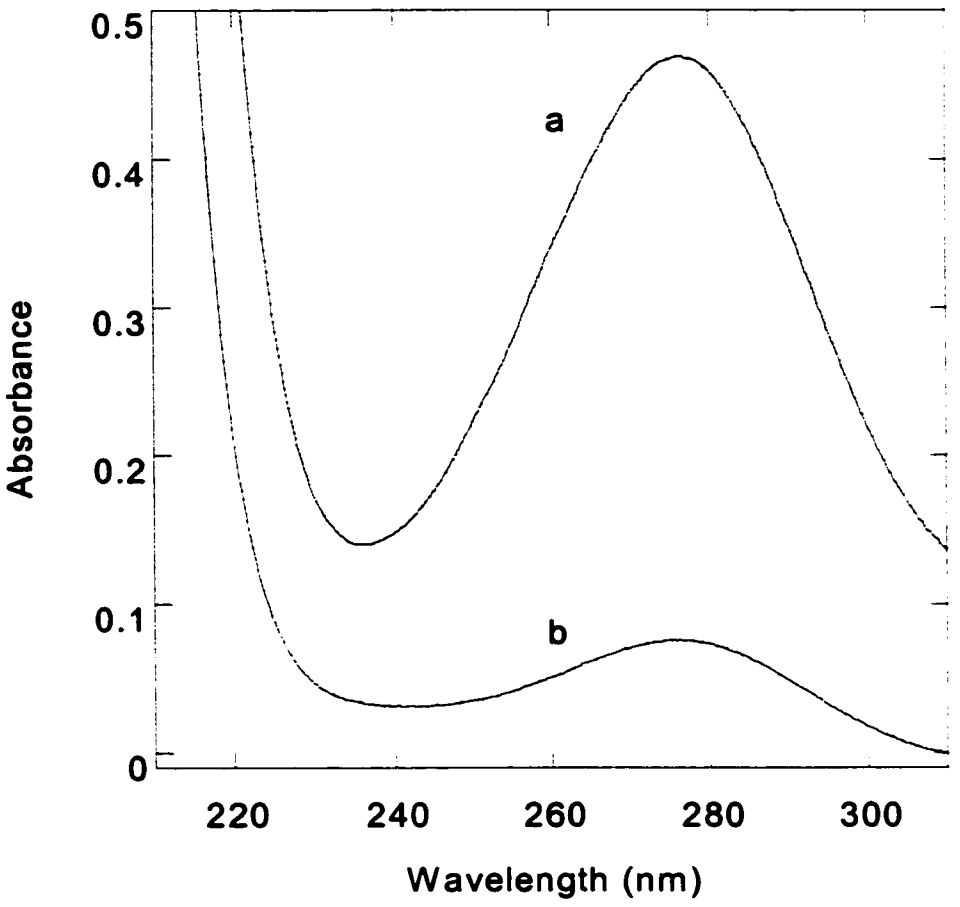

Figure 3.7. (a) UV spectrum recorded after the decomposition of 1.0 mM $Hg(SO_3)_2^{2-}$ at pH 3 and 45°C, in the presence of 20 μM free HSO_3^-; (b) spectrum of 1.0 mM HSO_3^- at pH 3. Both spectra were recorded in a 5 cm pathlength cell.

3.3 Discussion

3.3.1 Mechanism

The reduction of mercuric ion by excess aqueous sulfite in mildly acidic solutions was the subject of a previous report.[35] The values of the kinetic parameters a and b were measured at 25°C, and the unknown value of K_2 was estimated in order to extract individual rate constants. In agreement with that study, our results show that the rate of the reaction is inversely dependent on the concentration of uncoordinated S(IV), which exists mostly in the form HSO_3^- under the reaction conditions. Our measured value for b at 25°C, $(9 \pm 2) \times 10^{11}$ s M^{-1}, compares to $b = 4.3 \times 10^{11}$ s M^{-1} reported previously.[35]

As required by the inverse $[H^+]$ dependence of k_{obs}, the form of S(IV) which retards the reduction of the mercuric ion in acidic solution is SO_3^{2-} rather than HSO_3^-, although the concentration of the latter exceeds that of SO_3^{2-} by a factor of 10^4 at pH 3. We attribute the apparent lack of affinity of the mercuric ion for monoprotonated HSO_3^- to the structure of its major tautomer, in which the proton resides on S rather than on O.[42] Most HSO_3^- is thus not inclined to react with the mercuric ion, which is known to coordinate sulfite through the lone pair on S.[27]

Although the spectrum of the complex formed between the mercuric ion and excess sulfite in acidic solution is pH-dependent, the complex is most likely $Hg(SO_3)_2(H_2O)_n^{2-}$, rather than $Hg(SO_3)(SO_3H)^-$. The pK_a for SO_3H^- (protonated at O) has been estimated as 5.4.[42] Coordination of a proton-containing ligand to a metal complex generally lowers the pK_a, so that $Hg(SO_3)(SO_3H)^-$ is probably not formed in appreciable quantities even at the lowest pH (2) attained in this study.

The pK_a of 11.7 found in the spectrophotometric titration of $Hg(SO_3)_2^{2-}$ must therefore be attributed to another proton-containing ligand, most likely a coordinated water molecule such as that shown in eq 3.5. Furthermore, the ligand dissociation required by the observed kinetic behaviour of complex **IX** is of SO_3^{2-}, rather than SO_3H^-, which is inconsistent with the expected aquation behaviour of $Hg(SO_3)(SO_3H)^-$.

A mechanism which agrees with the experimental rate law for reduction of Hg(II) in the presence of excess hydrogen sulfite involves dissociation of sulfite from $Hg(SO_3)_2^{2-}$, followed by decomposition of $HgSO_3$, eq 3.7–3.8:

$$Hg(SO_3)_2^{2-}{}_{(aq)} \leftrightarrows HgSO_{3(aq)} + SO_3^{2-}{}_{(aq)} \qquad k_d, k_b \quad (3.7)$$

$$HgSO_{3(aq)} + n\,H_2O \rightarrow Hg^0{}_{(aq)} + HSO_4^-{}_{(aq)} + H^+ \qquad k_r \quad (3.8)$$

where k_d and k_b are rate constants for the dissociation of sulfite from $Hg(SO_3)_2^{2-}$ and the binding of sulfite to $HgSO_{3(aq)}$, respectively, and k_r is the rate constant for the water-assisted reduction of the mercuric ion by its coordinated sulfite ligand. Application of the steady-state approximation for the intermediate $HgSO_3$ yields the rate law:

$$-d[Hg(SO_3)_2^{2-}]/dt = k_d\,k_r\,[Hg(SO_3)_2^{2-}] / (k_b\,[SO_3^{2-}]_{free} + k_r) \qquad (3.9)$$

which reproduces the experimental rate law (including pseudo-first-order behaviour) with $a = k_d^{-1}$ and $b = k_b/k_dk_r$, *provided the formation of sulfite according to eq 3.7 does not cause the value of* $[SO_3^{2-}]_{free}$ *to change significantly.* Since k_r (45°C) = 0.134 s^{-1} is known from the previous chapter,[55] we calculate $K_2 = k_b/k_d = (1.68 \pm 0.07) \times 10^9$. Furthermore, $k_d = a^{-1} = 0.018 \pm 0.005\ s^{-1}$, which allows us to evaluate $k_b = (3.0 \pm 0.8) \times 10^7\ M^{-1}\ s^{-1}$.

Even kinetic experiments conducted under conditions where the sulfite released from $Hg(SO_3)_2^{2-}$ far exceeded the initial value of $[HSO_3^-]_{free}$ showed no appreciable deviation from pseudo-first-order behaviour. This behaviour was not

explained in a previous study.[35] Ligand dissociation from $Hg(SO_3)_2^{2-}$ in the first step of the mechanism (eq 3.7–3.8) ought to slow the decomposition reaction in most of our experiments, since this sulfite should increase the concentration of uncoordinated S(IV) as the reaction proceeds. However, no deviations from pseudo-first-order behaviour were observed. For example, decomposition of 0.93 mM $Hg(SO_3)_2^{2-}$ in a solution containing 0.11 mM uncoordinated HSO_3^- in 1.0 mM $HClO_4$ at 45°C generated a pseudo-first-order decay of absorbance at 230 nm, with k_{obs} = (0.0058 ± 0.00035) s^{-1}. Furthermore, values of k_{obs}^{-1} correlate with the initial concentration of uncoordinated [S(IV)], rather than the sum of this concentration and the sulfite released according to eq 3.7. Nonetheless, at the end of the reaction, the total titratable S(IV) is the sum of the both contributions.

The simplest explanation for this phenomenon is that the sulfite product liberated in eq 3.7 is unavailable for binding to the mercuric ion. The reaction shown in eq 3.10 accounts for the observed behaviour, kinetically masking the presence of one equiv. of sulfite while still permitting it to be titrated.

$$Hg^0_{(aq)} + HSO_3^-{}_{(aq)} + H^+ \leftrightarrows Hg{\cdot}SO_{2(aq)} + H_2O \qquad (3.10)$$

Although very little coordination chemistry of Hg^0 has been reported, SO_2 is well-known as a ligand to low-valent transition metal complexes and binds strongly on metallic surfaces. The formation of an SO_2 complex with Hg^0 is further consistent with the peak we observe in the product spectrum at 276 nm. The solubility of the putative $Hg{\cdot}SO_{2(aq)}$ must be at least three orders of magnitude greater than the solubility of Hg^0 in distilled water, (3.03 ± 0.12) x 10^{-7} M at 25°C.[10] This statement is based on the observation of pseudo-first-order kinetic behaviour even when $[Hg(SO_3)_2^{2-}]$ = 1.0 mM, since the final concentration of the proposed $Hg{\cdot}SO_2$ in this case is also 1.0 mM.

At temperatures below 45°C, the dissociation of sulfite from $Hg(SO_3)_2^{2-}$ is best described as a rapid preequilibrium preceding the rate-determining internal redox reaction of $HgSO_3$, since the y-intercepts of the plots of k_{obs}^{-1} vs. $[SO_3^{2-}]$ are not significant. However, at higher temperatures, a steady-state treatment of

the intermediate $HgSO_3$ is appropriate and the value of k_d can be estimated. The large value calculated for k_b is consistent with rapid capture of the sulfite ligand by $HgSO_3$.

3.3.2 Thermodynamic parameters

The form of the Eyring equation for the kinetic parameter b^{-1} is given in eq 3.11:

$$\ln (1/bT) = \ln(k_r/K_2T) = \ln(R/Nh) + (\Delta S_r^{\ddagger} - \Delta S_2^{0})/R - (\Delta H_r^{\ddagger} - \Delta H_2^{0})/RT \qquad (3.11)$$

where $\Delta S_r^{\ddagger}$ and $\Delta H_r^{\ddagger}$ are the entropy and enthalpy of activation for the redox reaction of $HgSO_3$, eq 3.8, and ΔS_2^{0} and ΔH_2^{0} are the entropy and enthalpy of binding of the second sulfite anion to $HgSO_3$. Since $\Delta H_r^{\ddagger}$ and $\Delta S_r^{\ddagger}$ have been measured independently as (105 ± 2) kJ/mol and (68 ± 6) J/mol·K, respectively,[55] the thermodynamic parameters for sulfite binding are ΔH_2^{0} = -(61 ± 2) kJ/mol and ΔS_2^{0} = -(17 ± 3) J/K·mol, such that ΔG_2^{0} = -(56 ± 10) kJ/mol at 25°C. This calculation permits an independent evaluation of K_2 from the temperature-dependence of k_{obs}, yielding $K_2 = 7 \times 10^9$ at 25°C, compared to 1.0×10^{10} obtained from the measured value of b at the same temperature (see above).

The sequential formation constants for mercuric ion-sulfite complexes have not previously been measured, however, modellers often use values estimated from the known value of β_2 and a K_1-K_2 correlation established for complexes of the mercuric ion with halides and other univalent anions.[57] From this relationship and $\beta_2 = 1.2 \times 10^{24}$ (18°C, μ = 0),[24] $K_1 = 5.0 \times 10^{12}$ and $K_2 = 2.5 \times 10^{11}$ were estimated, for a ratio $K_1/K_2 = 20$.[35] However, linear free energy relationships for univalent anions are not necessarily appropriate for divalent anions. For example, the first two sequential binding constants for carbonate anions to Hg^{2+} are 1.0×10^{11} and 3.1×10^3.[41] Using the reported value for β_2 at

298 K and μ=0.50 M of (2.1 ± 0.1) x 10^{23},[36] we can now derive K_1 = (2.1 ± 0.4) x 10^{13}. The values of ΔG_1^0, ΔH_1^0 and ΔS_1^0 can also be calculated from the reported values[36] for the overall formation of $Hg(SO_3)_2^{2-}$ and our derived values for the second binding of sulfite. All of the rate and equilibrium constants established for the mercuric ion-sulfite system are summarized in Table 3.3.

3.3.3 Speciation of mercuric ions

The distribution of mercuric ion-sulfite complexes can be determined using the formation equilibria as well as the acid-base equilibria for S(IV). The binding equilibria are given in eq 3.1-3.2 and the S(IV) acid base equilibria are found in eq 1.7-1.8.

The fraction of each mercuric ion-sulfite species present is its concentration divided by the sum of concentrations of all species. For example:

$$\alpha_{Hg^{2+}} = \frac{[Hg^{2+}]}{[Hg^{2+}]+[HgSO_3]+[Hg(SO_3)_2^{2-}]} \qquad (3.16)$$

where

$$\alpha_{Hg^{2+}} + \alpha_{HgSO_3} + \alpha_{Hg(SO_3)_2^{2-}} = 1 \qquad (3.17)$$

By substituting the equilibria expressions into eq 3.16, α-values can be determined from the binding constants:

$$\alpha_{Hg^{2+}} = \frac{1}{1+K_1[SO_3^{2-}]+K_1K_2[SO_3^{2-}]^2} \qquad (3.18)$$

Table 3.3. Summary of thermodynamic parameters for the aqueous mercuric ion – sulfite system

Reaction	K	ΔG° kJ/mol	ΔH° kJ/mol	ΔS° J/mol*K
$Hg^{2+} + 2\ SO_3^{2-} \rightarrow Hg(SO_3)_2^{2-}$	2.1×10^{23} [a]	-133	-91	141
$Hg^{2+} + SO_3^{2-} \rightarrow HgSO_3$	2.1×10^{13} [b]	-77	-30	158
$HgSO_3 + SO_3^{2-} \rightarrow Hg(SO_3)_2^{2-}$	10×10^{9} [c]	-56	-61	-17

$$\alpha_{HgSO_3} = \frac{K_1[SO_3^{2-}]}{1+K_1[SO_3^{2-}]+K_1K_2[SO_3^{2-}]^2} \quad (3.19)$$

$$\alpha_{Hg(SO_3)_2^{2-}} = \frac{K_1K_2[SO_3^{2-}]^2}{1+K_1[SO_3^{2-}]+K_1K_2[SO_3^{2-}]^2} \quad (3.20)$$

$[SO_3^{2-}]$ is calculated using eq 3.21:

$$[SO_3^{2-}] = [S(IV)]_{total} * \alpha_{SO_3^{2-}} \quad (3.21)$$

where $\alpha_{SO_3^{2-}}$ is given by:

$$\alpha_{SO_3^{2-}} = \frac{K_{a1}K_{a2}}{[H^+]^2+K_{a1}[H^+]+K_{a1}K_{a2}} \quad (3.22)$$

Using previously estimated sequential sulfite binding constants the major species was predicted to be the redox stable $Hg(SO_3)_2^{2-}$,[35] Figure 3.8, at pH 4 for all atmospherically relevant SO_2 concentrations. Our newly measured values for the sequential binding constants predict that at pH 4 the major species in water droplets in equilibrium with 0.1 ppb $SO_{2(aq)}$ (i.e. clean air) is the redox unstable $HgSO_3$, Figure 3.8. The major mercuric complex is not predicted to be $Hg(SO_3)_2^{2-}$ even when $P(SO_2)$ approaches 1 ppb (*i.e.* highly polluted air). The concentration of SO2 in water droplets in equilibrium with air can be calculated using Henry's Law constant, equation 1.6.

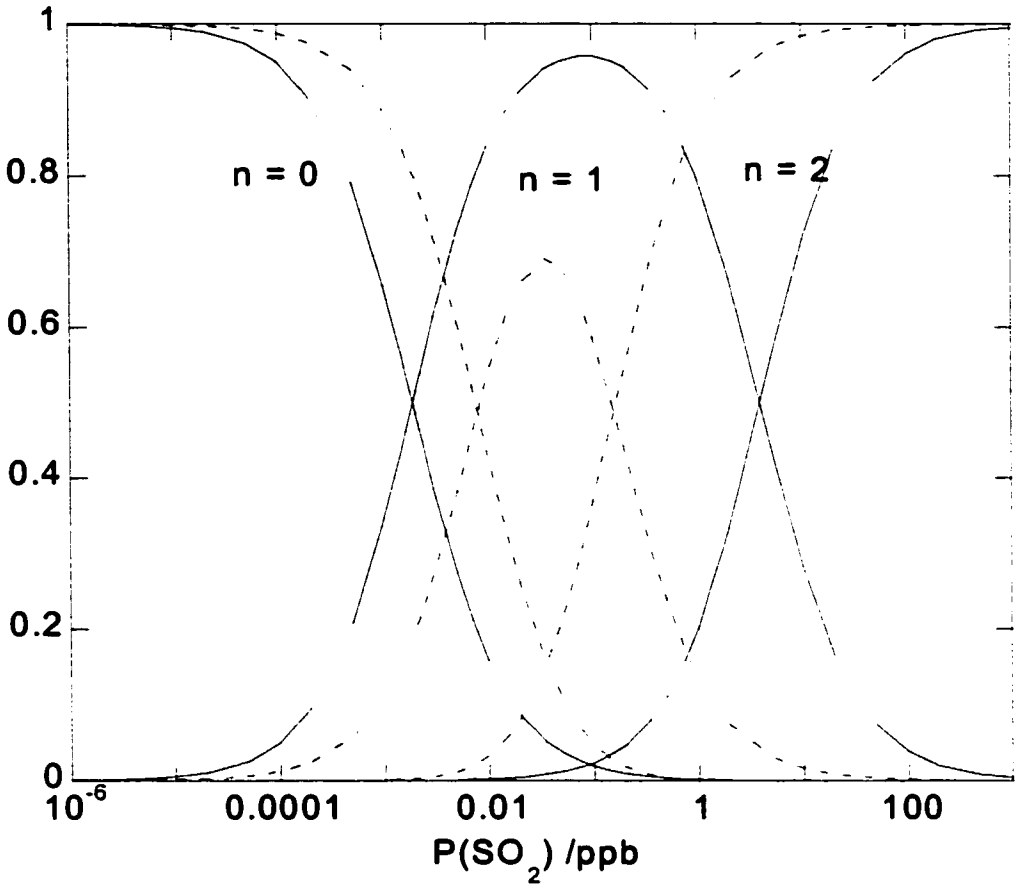

Figure 3.8. Speciation diagram for aqueous mercuric complexes Hg^{2+}, $HgSO_3$ and $Hg(SO_3)_2^{2-}$ at pH 4.0, in equilibrium with $SO_{2(g)}$. Solid lines: sequential binding constants determined in this work; dotted lines: binding constants determined previously.[35]

3.4 Conclusion

The aqueous sulfite ion reacts with $Hg^{2+}_{(aq)}$ to form 1:1 and 2:1 coordination complexes. The $Hg(SO_3)_2^{2-}$ complex is redox-stable. However, dissociation of a sulfite ligand forms redox-unstable $HgSO_3$. Under conditions where $Hg(SO_3)_2^{2-}$ predominates, the rate of reduction of the mercuric ion to Hg^0 by coordinated sulfite depends inversely on the concentration of uncoordinated sulfite, while it is unaffected by the amount of sulfite liberated by dissociation. Analysis of the kinetics yields the sequential sulfite binding constants $K_1 = 2.1 \times 10^{13}$ and $K_2 = 1.0 \times 10^{10}$ at $\mu = 0.10$ M. These values lead to the prediction that $HgSO_3$ is more abundant in clouds than $Hg(SO_3)_2^{2-}$ under virtually all atmospheric conditions. The product of the redox reaction appears to be a strongly-bound $Hg^0 \cdot SO_2$ complex, which is at least three orders of magnitude more soluble than uncomplexed $Hg^0_{(aq)}$. This finding may have important implications for the partitioning of atmospheric mercury from the gas phase into atmospheric water droplets prior to its wet deposition.

Chapter 4

General Conclusions

4.1 Thermodynamic parameters

Previously estimated thermodynamic parameters have now been measured or derived for the aqueous mercuric ion-sulfite system and are summarized in Table 3.3. The new values for the sequential sulfite binding constants lead to significantly different predictions for the speciation of mercuric ions in pH 4.0 clouds, compared to previous estimates.[35] Using the new binding constants, the major mercuric ion species in water droplets in equilibrium with 0.1 ppb $SO_{2(g)}$ (*i.e.*, clean air) is now predicted to be unstable $HgSO_3$, which undergoes reduction to Hg^0 with a half-life of approximately one minute at 25°C. The major mercuric complex is not predicted to be stable $Hg(SO_3)_2^{2-}$, even when $P(SO_2)$ approaches 1 ppb (highly polluted air).

In order to properly predict Hg chemistry in water droplets, speciation in the presence of several anions must be considered. Chloride is commonly found in atmospheric water. In the marine boundary layer, its concentration (expressed as HCl) is 100 – 300 pptv.[17] Concentrations are typically lower over land, but values of up to a few ppb can be found in rainwater near urban areas.[17] In the presence of chloride, the complexes $Hg(Cl)_n^{2-n}$ are formed. Using the equilibrium constant for the binding of two Cl^- to Hg^{2+}, $K = 10^{14}$ M^2,[21] and previously determined binding constants for $Hg(SO_3)_n^{2-2n}$,[35] $HgCl_2$ was predicted to be the major species in cloud and fog droplets for a HCl concentration of 1 $\mu g/m^3$ at pH 4.[21] Since the presence of chloride complexes diminishes the ability of sulfite to reduce Hg(II), the rate of deposition is predicted to increase.

Using our newly determined first and second binding constants for sulfite to mercuric ion and an HCl concentration of 1 ppt at pH 4, we calculate that $HgCl_2$ does not form in any appreciable amount, Figure 4.1. Even when the chloride concentration is increased 1000-fold, $HgCl_2$ constitutes less than 10% of the Hg^{2+} species. Clearly, the magnitude of the binding constants greatly affects models simulating cloud equilibria.

Our investigations further show a very strong temperature effect on the reduction of $HgSO_3$ to Hg^0 and S(VI). Current models do not include temperature as a variable. The redox decomposition of $HgSO_3$ at 25°C has a half-life of approximately one minute, while at 6.6°C its half-life is approximately 20 minutes. Assuming $HgSO_3$ is the major species in clouds, its reduction, and therefore the concentration of mercuric ion in rain droplets is highly temperature-dependent. In warmer regions, Hg^{2+} will be rapidly reduced to Hg^0, which will partition into the gas phase, resulting in less mercury in the precipitation. In colder climates, the reduction will be much slower and so, more mercury will be deposited.

4.2 Sulfite solubilization of Hg(0)

It is possible that the formation of $Hg{\cdot}SO_{2(aq)}$, either by direct reaction of Hg^0 with hydrogen sulfite, or by reduction of aqueous Hg(II) in the presence of excess sulfite, has an important effect on the deposition rate for atmospheric Hg. Due to the high solubility of the Hg^0 complex, it is not necessary to suppose that the major form of mercury in rain is Hg(II). If $Hg{\cdot}SO_2$ is as soluble as we believe ($\geq$1 mM) then oxidation to Hg^{2+} is no longer required to explain the discrepancy between the amount of mercury predicted to be in cloud droplets and the concentrations actually observed.

Formation of $Hg{\cdot}SO_2$ could occur in the gas phase where both partners are present followed by dissolution into cloud droplets for deposition. A decrease in lake mercury for which the only input was atmospheric deposition was reported[58] to parallel a similar decrease in sulfate. It is possible that as less SO_2 is emitted

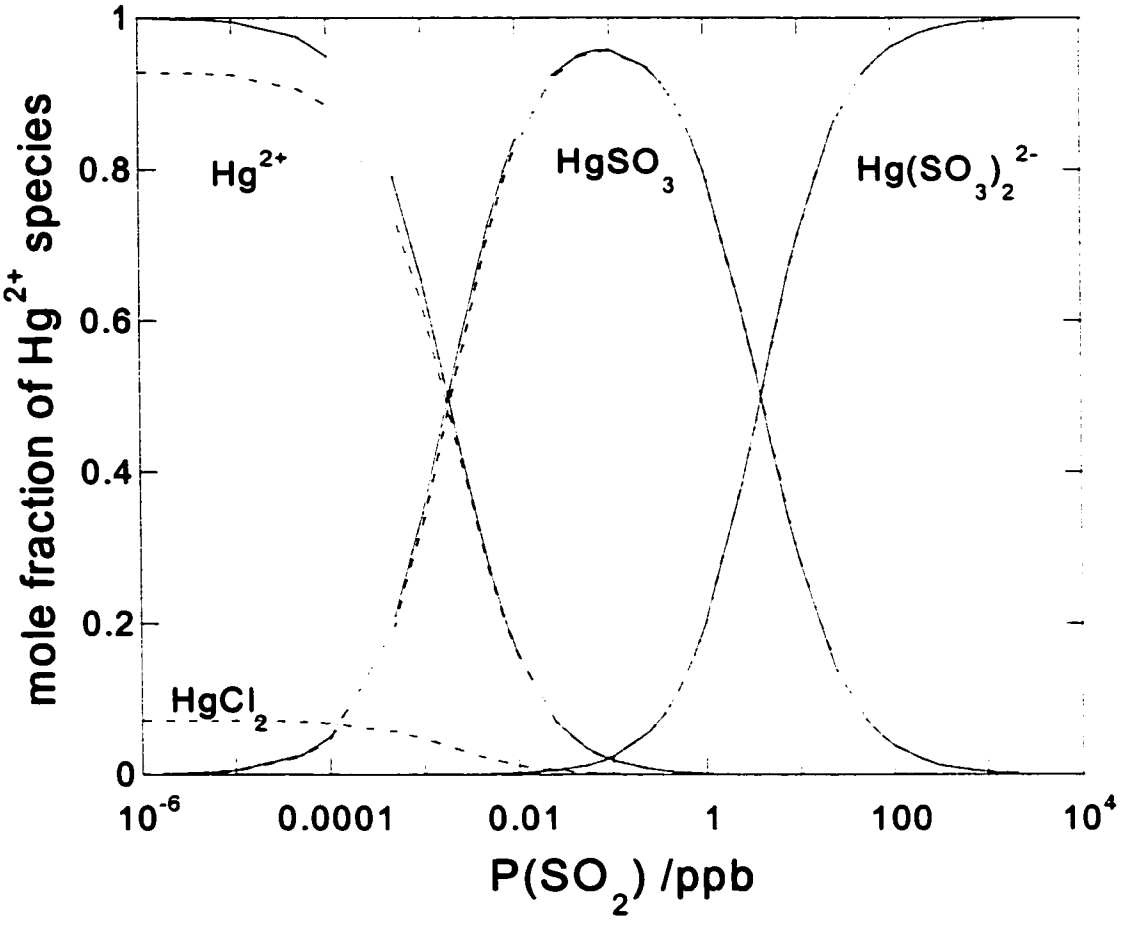

Figure 4.1. Speciation diagram for aqueous mercuric complexes Hg^{2+}, $HgSO_3$, $Hg(SO_3)_2^{2-}$, and $HgCl_2$ at pH 4.0, in equilibrium with $SO_{2(g)}$. The solid lines: [HCl] = 1 ppt; dotted lines [HCl] = 1 ppb.

as industrial waste, the formation of $Hg{\cdot}SO_2$ in the gas phase decreases, and less mercury partitions into atmospheric water droplets. However, since there is little precedent for coordination chemistry of Hg(0), more work will be required to provide a convincing characterization of this potentially important new species.

Chapter 5

Experimental

5.1 Preparation and standardization of mercury(II) solutions

Mercury(II) oxide (Aldrich, 99.999%) was dissolved in concentrated perchloric acid and diluted with deionized ("milli-q plus") water to produce stock solutions of approximately 0.05 M Hg^{2+} in 0.2 M $HClO_4$. Solutions were standardized upon preparation by sodium thiocyanate titration using ferric alum indicator. The indicator is a saturated solution of ferric ammonium sulfate in water to which a few drops of 6 M nitric acid are added. For the titration, 5 mL of the mercury solution, 1 mL of 6 M nitric acid, and a few drops of the indicator are mixed together. The titration proceeds as follows:

$$Hg(SCN)^{+} + SCN^{-} \leftrightarrows Hg(SCN)_2 \quad (5.1)$$

$$Hg^{2+} + Hg(SCN)^{+} \leftrightarrows 2\ Hg(SCN)^{+} \quad (5.2)$$

$$Fe^{3+} + SCN^{-} \rightarrow Fe(SCN)^{2+} \quad (5.3)$$

$Hg(SCN)^{+}$ is a soluble compound but $Hg(SCN)_2$ is insoluble. Near the endpoint, when there are no longer free mercuric ions in solution, $Hg(SCN)_2$ precipitates as colourless needles. The precipitate does not interfere with the sharp colour change at the endpoint from colourless to reddish-brown. Stock mercuric ion solutions were diluted with milli-q water to the desired concentration for use in kinetics experiments.

5.2 Preparation and standardization of sulfite solutions

Approximately 0.1 M sulfite solutions were prepared daily by dissolving sodium sulfite in deionized water. The exact concentration was determined by iodometric titration with sodium thiosulfate. 0.1 M sodium thiosulfate solutions were prepared monthly by dissolving the salt in 500 mL of milli-q water. Stock solutions of approx 0.05 M triiodide were prepared by dissolving 0.12 mol I_2 (Aldrich, ACS reagent, 99+%) and 0.05 mol KI (Aldrich, 99+% ACS reagent) in 500 mL of milli-q water. The I_3^- solution was standardized by thiosulfate. A 0.5% starch indicator solution was prepared weekly. Enough triiodide was added to 10 mL of sulfite solution so that a small excess (ca. 20%) remained after complete reaction. The endpoint is indicated by a colour change from blue to clear. Triiodide reacts with sulfite and thiosulfate according to equations 5.4-5.5.

$$SO_3^{2-} + I_3^- + H_2O \rightarrow SO_4^{2-} + 3\ I^- \quad (5.4)$$

$$I_3^- + 2\ S_2O_3^{2-} \rightarrow 3\ I^- + S_4O_6^{2-} \quad (5.5)$$

Sulfite is susceptible to trace-metal catalyzed autoxidation. Air-free working solutions were prepared daily. Argon-saturated solutions were prepared by bubbling with argon. A chromous tower was used to remove oxygen from the argon. To prepare the chromous solution, Zn(s) (Fisher) was used to reduce a solution of approx 0.1 M Cr(III) (BDH AnalaR Reagent) in 1 M HCl.

5.3 Preparation of Hg_2^{2+} solutions

A drop of Hg^0 (Puratronic, 99.999995%) was placed in a solution of 1 mM Hg^{2+} and stirred overnight, followed by decantation of the aqueous phase. The concentration of Hg_2^{2+} was calculated from its absorbance at 236 nm (ϵ = 2.8 x 10^4 M^{-1} cm^{-1}).[37, 38]

5.4 Other reagents

Perchloric acid solutions were prepared by diluting the concentrated acid (Analar, 70%) to the desired concentration with distilled deionized water. Sodium perchlorate solutions were prepared by dissolving the salt (Aldrich, 99% ACS Reagent) in milli-q water.

5.5 Procedure for kinetics experiments

Distilled deionized water, perchloric acid, and mercury(II) solutions were transferred by all-glass syringes into a 3 mL, 10 mm pathlength square or round quartz cuvette capped with a white rubber septum (Aldrich). The cuvette was placed in the thermostatted cell compartment of a Cary 100 spectrophotometer for a minimum of 15 minutes while the temperature was regulated (± 0.1 °C) with a circulating water bath. To initiate the reaction, sulfite was added using syringe-septa techniques The absorbance at the appropriate wavelength was monitored as a function of time.

Air-free experiments were performed by bubbling Cr-scrubbed argon through the solution in the cuvette for 15 minutes before placing the cuvette in the sample compartment.

5.6 Extinction coefficient measurements

The extinction coefficient of $HgSO_3$ was measured by mixing Hg(II), $HClO_4$ and water in a 10 mm cuvette and thermostatting to 15 °C. Sulfite was added and the spectrum was recorded immediately at a scan rate of 300 nm/min.

The extinction coefficient of Hg_2^{2+} was measured by mixing an excess of Hg(II) with S(IV) at pH 3 and allowing the reaction to proceed to completion at room temperature (approx 15 min). The spectrum was then recorded at a scan rate of 300 nm/min.

The extinction coefficient of $Hg(SO_3)_2^{2-}$ was measured by mixing Hg(II), $HClO_4$ and water in a 10 mm cuvette at room temperature. . Sulfite was added and the spectrum was recorded immediately at a scan rate of 300 nm/min.

5.7 Spectrophotometric titration

A mercuric ion solution was deaerated with Ar in a three-necked flask, then cooled to approximately 5°C. Sulfite solution was added, followed by enough $NaOH_{(s)}$ to raise the pH to 13. Following addition of each aliquot of $HClO_4$, the pH was measured using a Corning 430 pH meter. A 3 mL sample was removed by syringe in order to record its UV spectrum. Absorbance readings at 230 nm were all normalized to the initial $Hg(SO_3)_2^{2-}$ concentration.

References

(1) Swain, E. B.; Engstrom, D. R.; Brigham, M. E.; Henning, T. A.; Brezonik, P. L. *Science* **1992**, *257*, 784-787.

(2) Vandal, G. M.; Fitzgerald, W. F.; Boutron, C. F.; Candelone, J.-P. *Nature* **1993**, *362*, 621-623.

(3) Martinez-Cortizas, A.; Pontevedra-Pombal, X.; Garcia-Rodeja, E.; Novoa-Munoz, J. C.; Shotyk, W. *Science* **1999**, *284*, 939-942.

(4) Glass, G. E.; Sorensen, J. A. *Environ. Sci. Technol.* **1999**, *33*, 3303-3312.

(5) Porcella, D. B. In *Mercury Pollution Integration and Synthesis*; CRC Press Inc.: Ann Arbor, 1994; pp 3-19.

(6) Mason, R. P.; Fitzgerald, W. F.; Morel, F. M. *Geochimica et Cosmochimica Acta.* **1994**, *58*, 3191-3198.

(7) Schroeder, W. H.; Munthe, J. *Atmos. Environ.* **1998**, *32*, 809-822.

(8) Slemr, F.; Langer, E. *Nature* **1992**, *355*, 434-437.

(9) Lindberg, S. E.; Stratton, W. J. *Environ. Sci. Technol.* **1998**, *32*, 49-57.

(10) Clever, H. L.; Johnson, S. A.; Derrick, M. E. *J. Phys. Chem.* **1985**, *14*, 631-680.

(11) Hall, B. *Water Air Soil Pollut* **1995**, *80*, 301-315.

(12) Schroeder, W. H.; Yarwood, G.; Niki, H. *Water Air Soil Pollut.* **1991**, *56*, 653-666.

(13) Iverfeldt, A.; Lindqvist, O. *Atmos. Environ.* **1986**, *20*, 1567-1573.

(14) McElroy, W. J.; Munthe, J. *Acta Chem Scand* **1991**, *45*, 254-257.

(15) Munthe, J. *Atmos. Environ.* **1992**, *26A*, 1461-1468.

(16) Tokos, J. J. S.; Hall, B.; Calhoun, J. A.; Prestbo, E. M. *Atmos. Environ.* **1998**, *32*, 823-827.

(17) Brasseur, G. P.; Orlando, J. J.; Tyndall, G. S. *Atmospheric Chemistry and Global Change*; Oxford University Press: New York, 1999.

(18) Yamamoto, M. *Chemosphere* **1995**, *32*, 1217-1224.

(19) Lin, C.; Pehkonen, S. O. *J. Geophys. Res.* **1998**, *103*, 28093-28102.

(20) Armstrong, A. M.; Halpern, J. *Can. J. Chem.* **1957**, *35*, 1020-1030.

(21) Seigneur, C.; Wrobel, J.; Constantinou, E. *Environ. Sci. Technol.* **1994**, *28*, 1589-1597.

(22) Lelieveld, J.; Roelofs, G. J.; Ganzeveld, L.; Feichter, J.; Rodhe, H. *Phil. Trans. Royal Soc. London B* **1997**, *352*, 149-158.

(23) Brandt, C.; van Eldik, R. *Chem. Rev.* **1995**, *95*, 119-190.

(24) Smith, R. M.; Martell, A. E. *Critical Stability Constants*; Plenum: New York, 1976; Vol. 4.

(25) Bishenden, E.; Donaldson, D. J. *J. Phys. Chem.* **1998**, *102*, 4638-4642.

(26) Ermakov, A. N.; Poskrebyshev, G. A.; Purmal, A. P. *Kinet. Catal.* **1997**, *38*, 295-308.

(27) Newman, G.; Powell, D. P. *Spectrochim. Acta* **1963**, *19*, 213-224.

(28) Hall, J. P.; Griffith, W. P. *Inorg. Chim. Acta* **1981**, *48*, 65-71.

(29) Spitzer, U.; van Eldik, R. *Inorg. Chem.* **1982**, *21*, 4008-4014.

(30) Koshy, K. C.; Harris, G. M. *Inorg. Chem.* **1983**, *22*, 2947-2953.

(31) Johnson, M. D.; Bernard, J. *Inorg. Chem.* **1992**, *31*, 5140-5142.

(32) Sarala, R.; Stanbury, D. M. *Inorg. Chem.* **1990**, *29*, 3456-3460.

(33) Siskos, P. A.; Peterson, N. C.; Huie, R. E. *Inorg. Chem.* **1984**, *23*, 1134-1137.

(34) Berglund, J.; Elding, L. I. *Inorg. Chem.* **1995**, *34*, 513-519.

(35) Munthe, J.; Xiao, Z. F.; Lindqvist, O. *Water Air Soil Pollut.* **1991**, *56*, 621-630.

(36) Marsicano, F.; Hancock, R. D. *J. Coord. Chem.* **1976**, *6*, 21-29.

(37) Higginson, W. C. E. *J. Chem. Soc.* **1951**, 1438.

(38) Fujita, S.; Horii, H.; Taniguchi, S. *J. Phys. Chem.* **1973**, *77*, 2868-2871.

(39) Espenson, J. H. *Chemical Kinetics and Reaction Mechanisms*; McGraw-Hill: New York, 1981.

(40) Morse, P. M.; Spencer, M. D.; Wilson, S. R.; Girolami, G. S. *Organometallics* **1994**, *13*, 1646-1655.

(41) Bilinski, H.; Markovic, M.; Gessner, M. *J. Am. Chem. Soc.* **1980**, *19*, 3440-3443.

(42) Guthrie, J. P. *Can. J. Chem.* **1979**, *57*, 454-457.

(43) Hayon, E.; Treinin, A.; Wilf, J. *J. Am. Chem. Soc* **1972**, *94*, 47-57.

(44) Pai, P.; Karamchandani, P.; Seigneur, C. *Atmos. Environ.* **1997**, *31*, 2717-2732.

(45) Wilmarth, W. K.; Stanbury, D. M.; Byrd, J. E.; Po, H. N.; Chua, C.-P. *Coord. Chem. Rev.* **1983**, *51*, 155-179.

(46) Simandi, L. I.; Jaky, M.; Schelly, Z. A. *J. Am. Chem. Soc.* **1984**, *106*, 6866-6867.

(47) Douglas, J. E.; Kenyon, G. L.; Kollman, P. A. *Chem. Phys. Lett.* **1978**, *57*, 553-556.

(48) Douglas, J. E.; Kollman, P. A. *J. Am. Chem. Soc.* **1978**, *100*, 5226-5227.

(49) Sakaki, S.; Sato, H.; Imai, Y.; Morokuma, K.; Ohkubo, K. *Inorg. Chem.* **1985**, *24*, 4528-4544.

(50) Kolb, C. E.; Jayne, J. T.; Worsnop, D. R. *J. Am. Chem. Soc.* **1994**, *116*, 10314-10315.

(51) Phillips, J. A.; Canagaratna, M.; Goodfriend, H.; Leopold, K. R. *J. Phys. Chem.* **1995**, *99*, 501-504.

(52) Morokuma, K.; Muguruma, C. *J. Am. Chem. Soc.* **1994**, *116*, 10316-10317.

(53) Hoffmann, M.; von Ragué Schleyer, P. *J. Am. Chem. Soc* **1994**, *116*, 4947-4952.

(54) Munthe, J. *Atmos. Environ.* **1992**, *26A*, 553-557.

(55) Van Loon, L.; Mader, E.; Scott, S. L. *J. Phys. Chem. A* **2000**, *104*, 1621-1626.

(56) Martin, L. R. In *SO_2, NO and NO_2 Oxidation Mechanisms: Atmospheric Considerations*; Calvert, J. G., Ed.; Butterworth Publishers, 1984; Vol. 3, pp 63-100.

(57) Dyrssen, D.; Wedborg, M. *Water Air Soil Pollut.* **1991**, *56*, 507-519.

(58) Watras, C. J.; Morrison, K. A.; Hudson, R. J. M.; Frost, T. M.; Kratz, T. K. *Environ. Sci. Technol.* **2000**, *34*, 4051-4057.

List of publications

Lisa Van Loon, Elizabeth Mader, and Susannah L. Scott, "Reduction of the Aqueous Mercuric Ion by Sulfite: UV Spectrum of $HgSO_3$ and its Intramolecular Redox Reaction", *J. Phys. Chem. A*, **2000**, *104*, 1621-1626.

Lisa L. Van Loon, Elizabeth A. Mader, and Susannah L. Scott, "Sulfite Stabilization and Reduction of the Aqueous Mercuric Ion: Kinetic Determination of Sequential Formation Constants", *J. Phys. Chem. A*, **2001**, 105, 3190-3195.